THE ASTROPHYSICAL JOURNAL, 446:203–227, 1995 June 10

THE LITHIUM DIP IN M67: COMPARISON WITH THE HYADES, PRAESEPE, AND NGC 752 CLUSTERS

SUCHITRA BALACHANDRAN[1]
Department of Physics and Astronomy, University of North Carolina; and Department of Astronomy, Ohio State University, 174 West 18th Avenue, Columbus, OH 43210; suchitra@payne.mps.ohio-state.edu
Received 1994 May 16; accepted 1994 November 29

ABSTRACT

Lithium abundances were measured in 17 subgiants and giants which have evolved from the main-sequence Li dip in the old open cluster M67. The absence of detectable Li in all but one subgiant argues strongly that Li is severely destroyed, not merely diffused from observable view, in the main-sequence stars. A comparison with the Hyades, Praesepe, NGC 752, and M67 clusters is performed, requiring the adoption of a uniform temperature calibration, the use of newly standardized photometry for NGC 752, and the rederivation of Li abundances from published equivalent widths. Limitations of the commonly used temperature calibrations, and our adopted choice of the Saxner & Hammarbäck (1985) calibration, are discussed. Adoption of this calibration results in a significant change in the shape of the Hyades dip.

A comparison of the Li dips in the various clusters reveals intriguing details. The mass at the Li dip depends upon the metallicity of the stars, but the zero-age main-sequence (ZAMS) temperatures of the dip stars are found to be independent of their metallicity. The morphology of the Li dip is characterized by a sharp drop at the blue edge and a more gradual rise at the red edge. There is no change in the ZAMS temperature or shape of the blue edge with age. The red edge becomes less steep with age; this may either be due to the evolution of the Li dip, or be caused by a decrease in Li in stars cooler than the red edge and thus unrelated to the Li dip phenomenon. The Li versus effective temperature distributions in the Hyades and Praesepe clusters, which are of the same age but different metallicity, are found to be identical in both the F and G dwarfs.

None of the models so far proposed adequately explains the data. Microscopic diffusion and mass loss are contradicted by the observations of the Li dip. Models which incorporate rotation produce the Li dip through meridional circulation, turbulence, or rotational braking. Meridional circulation is in conflict with observations of Li outside the Li dip. All of the rotation models would produce a larger scatter in the Li dip than is observed. Observations suggest that the stars in the Li dip may undergo spin-down on a much longer timescale than late-F and G dwarfs. Examination of the rotational velocity distribution in dip stars in a cluster older than the Hyades may provide a clue to the anomalous mixing and Li depletion in the dip stars.

Subject headings: open clusters and associations: individual (M67) — stars: abundances — stars: interiors

1. INTRODUCTION

In the earliest measurements of Li in Hyades F stars, Wallerstein, Herbig, & Conti (1965) were only able to place upper limits on the [Li/Ca] abundances of several stars around $B-V = 0.4$. Constrained by the sensitivity of photographic plates, their upper limits were at most a factor of 6 below detections, yet this scatter in Li raised comment in their study. Three possible reasons were discussed, most interesting among them destruction related to rotation. It was not until more sensitive Reticon detectors became available, and the Hyades cluster was reobserved, that Boesgaard & Tripicco (1986) determined that Li abundances in these stars were a factor of 30 or more lower than in hotter and cooler stars. This drop in the Li abundance, the Li dip, is confined to a 300 K range in effective temperature around 6600 K. The dip has since been seen in a large number of clusters 200 Myr and older, and in field stars.

Many of the theoretical explanations for Li depletion on the main sequence have been able to account for the Li dip. This is in large part because the temperature at the dip roughly divides stars with and without surface convective zones, and hence those that do and do not undergo rotational spin-down, thus providing a number of free parameters to the imaginative theorist. While the various models are able to explain the surface depletion of Li in these stars using different physical mechanisms and stellar properties, they make different predictions for the interior composition of the star. The oldest cluster in which the Li dip has been documented is the 2 Gyr old cluster NGC 752 (Hobbs & Pilachowski 1986a; Pilachowski & Hobbs 1988). At this age the dip stars are still on the main sequence. By the age of M67 (4–5 Gyr), the Li dip stars have evolved off the main sequence. The convective envelopes of the subgiants and giants in M67 have deepened and dredged up material from the interior of the stars and thus provide a view of the internal composition. The subgiant and giant branch is well populated and provides the ideal hunting ground for the search for clues to the cause of the Li dip. In order to distinguish between the various models which purport to explain the Li dip, an understanding of the evolution of the dip with age, and the effects of other parameters, e.g., metallicity, are vital. With the inclusion of M67, published cluster data now

[1] Visiting Astronomer, Kitt Peak National Observatory and Cerro Tololo Inter-American Observatory, National Optical Astronomy Observatories, operated by the Association of Universities for Research in Astronomy, under contract with the National Science Foundation; Guest Observer, McDonald Observatory, University of Texas at Austin.

cover ages between 50 Myr and 5 Gyr, and metallicities between [Fe/H] = −0.15 and +0.15, thus providing an adequate database for an extensive comparison.

We present new observations of subgiants and giants in M67 in § 2. An examination of the published cluster analyses showed that effective temperatures have been determined using a variety of calibrations and techniques used to determine Li abundances vary considerably. Cluster comparisons required a complete reanalysis to a uniform standard. The calibration adopted, its limitations, comparisons with other calibrations, and the rederived temperatures and Li abundances are presented in § 3. The clusters are compared with each other in § 4, and with theoretical models in § 5. The results of this study are summarized in § 6.

2. NEW OBSERVATIONS AND ANALYSIS

Seventeen subgiants and giants were observed in the old open cluster M67. The stars are identified by their Sanders (1977) numbers which are cross-referenced to either the Fagerholm (1906) or Eggen & Sandage (1964) numbers (Table 1). The data were gathered at a variety of sites as detailed in Table 1. The subgiants were mainly observed with the 4 m telescope at Cerro Tololo Inter-American Observatory (CTIO) in 1989 March and May. The Cassegrain echelle spectrograph with the air Schmidt camera and GEC CCD detector yielded a 2 pixel resolution of ∼0.39 Å at 6700 Å. The giants were observed with the 4 m telescope at KPNO in 1991 November. The Cassegrain echelle spectrograph with the UV fast camera and the smaller pixel-sized TI 800 × 800 CCD detector gave a higher 2 pixel resolution of ∼0.24 Å. One giant, F135, was observed with the cross-dispersed coudé echelle spectrograph (Tull et al. 1994) and TI 800 × 800 CCD detector at the 2.7 m telescope at McDonald Observatory in 1992 November, which gave a much higher 2 pixel resolution of ∼0.15 Å. Spectra of four stars at the base of the red giant branch and a second spectrum of one giant were acquired at the KPNO 4 m telescope in 1994 January with the echelle spectrograph, the red long focus camera, and the Tek 2048 × 2048 chip to yield a 2 pixel resolution of 0.16 Å. Typically S/N's between 75 and 100 were obtained for each star. The data were reduced using standard IRAF routines. Th-Ar lamp spectra were used to establish the wavelength scale.

The effective temperatures of the stars were obtained from broadband colors. $B-V$ colors were taken from Eggen & Sandage (1964) and $V-K$ colors from Cohen, Frogel, & Persson (1978). A reddening of $E(B-V) = 0.04$ was adopted for the cluster as recommended by Nissen, Twarog, & Crawford (1987) from their extensive analysis of Strömgren photometry. Based on the interstellar extinction relationship of Mathis (1990), this corresponds to $E(V-K) = 0.11$. Effective temperatures were derived from $B-V$ colors using the calibration of Böhm-Vitense (1981) and from $V-K$ colors using the empirical calibration of Ridgway et al. (1980). When both $B-V$ and $V-K$ colors were available, the average temperature was adopted, and these are listed in Table 1. For the two warmest stars in our sample, the turn-off stars F111 and F115, effective temperatures were also determined using the $B-V$ calibration of Saxner & Hammarbäck (1985, hereafter SH) with [Fe/H] = 0.0. The agreement with the Böhm-Vitense (1981) calibration was found to be excellent. Gravities were estimated from the effective temperatures and bolometric magnitudes, assuming a distance modulus $m-M = 9.60$ (Nissen et al. 1987) and a turn-off mass of 1.2 $M_\odot$ (Demarque, Green, & Guenther 1992). The nearest available gravity in the Bell et al. (1976) and Bell, Eriksson, & Gustafsson (1990) model atmosphere grid was adopted for each star and is listed in Table 1. The microturbulent velocity of 1.7 km s^{-1} was adopted for all stars.

Lithium abundances were derived by fitting a synthetic spectrum to a 10 Å region around the Li I doublet at 6707.8 Å. Model atmospheres from the grid of Bell et al. (1976, 1990) and the LTE synthesis program MOOG (Sneden 1973) were used in the analysis. The wavelengths of the atomic lines in the region were obtained from the compilation of Kurucz & Pey-

TABLE 1

NEW OBSERVATIONS: TEMPERATURES, GRAVITIES, AND Li ABUNDANCES IN M67

Sanders	V	$B-V$	$V-K$	$T_{\rm eff}$ (K)	log g	log ϵ(Li)	W_λ(Li)[a] (mÅ)	ID
794[b].....	12.89	0.98	2.23	5000	3.75	<0.5	<6	IV-77
978[c].....	9.72	1.38	2.99	4125	2.25	<−0.5	<12	F108
986[d].....	12.74	0.56	...	6205	3.75	<1.9	<11	F111
989[e].....	11.45	1.06	...	4740	3.00	<0.0	<4	F135
1001[b].....	12.40	0.99	2.31	4905	3.75	<0.5	<8	I-17
1010[c].....	10.48	1.11	2.33	4640	3.00	<0.4	<11	F141
1016[c].....	1030	1.26	2.67	4375	2.25	<−0.2	<9	F105
1034[d].....	12.65	0.63	1.32	5950	3.75	<1.6	<8	F115
1231[b].....	12.93	0.93	2.17	5045	3.75	<0.5	<6	II-22
1239[d].....	12.77	0.76	...	5550	3.75	<1.1	<7	F226
1250[b].....	9.69	1.36	3.09	4010	2.25	<−1.0	<8	F170
1254[c].....	11.50	1.05	2.23	4760	3.00	<0.4	<9	F231
1279[c].....	10.55	1.13	2.38	4700	3.00	<0.5	<12	F164
1288[c].....	11.32	1.09	2.39	4760	3.00	<0.4	<9	III-34
1293[c].....	12.16	1.02	...	4830	3.75	<0.6	<10	III-35
1305[d].....	12.26	1.02	2.14	4830	3.75	<0.6	<10	F193
1463[c].....	12.94	1.01	...	4850	3.75	1.0	25	III-57
1463[b].....	12.94	1.01	...	4850	3.75	0.85	20	III-57

[a] Equivalent width derived from the stellar synthesis.
[b] Observed at KPNO with Cassegrain echelle spectrograph + red long focus camera + Tek CCD.
[c] Observed at KPNO with Cassegrain echelle spectrograph + UV fast camera + TI CCD.
[d] Observed at CTIO with Cassegrain echelle spectrograph + air Schmidt camera + GEC CCD.
[e] Observed at McDonald Observatory with coudé echelle spectrograph + TI CCD.

tremann (1975), and "solar" *gf*-values were derived by matching a synthetic spectrum with $T_{\rm eff} = 5750$ K, log $g = 4.5$, and the Anders & Grevesse (1989) solar elemental mixture with C, N, and O updates from Grevesse et al. (1991, 1990) and Grevesse & Noels (1993), respectively, to the observed solar spectrum. The wavelengths, excitation potentials, and *gf*-values of the CN lines in the region were taken from Gilroy (1988). The *gf*-values and wavelengths of the ^{7}Li I doublet are listed in Andersen, Gustafsson, & Lambert (1984) and are based on a radiative lifetime measurement (Gaupp, Kuste, & Andra 1982). The ^{6}Li contribution, which should be negligible in stars which have undergone even small amounts of ^{7}Li depletion and is estimated to be at most 8% in Population I stars which have not undergone any ^{7}Li depletion (Lemoine et al. 1993), was not included in the analysis.

Synthetic spectra were calculated using the appropriate model atmosphere parameters for each star, and the Li abundance was varied to obtain a good fit to the observed spectrum. The solar abundance was assumed for all other elements, and the consistently good match to the Fe I features in this region lends credence to our temperature, gravity, and microturbulence estimates. With the exception of one star, Li was not detected in any of the subgiants or giants; the synthetic fits yielded upper limits to the Li abundance. The typical equivalent width of a noise feature is estimated from the S/N's of 75–100 and 2 pixel resolution of 0.15–0.30 Å to range between 2 and 5 mÅ. Our synthetic fits to the Li I feature were conservatively placed at twice the equivalent width of a typical noise feature. Additional uncertainty is introduced because the Li I feature is blended with the Fe I λ6707.4 line which dominates the blend at cooler temperatures especially when the Li I contribution is small. The upper limits to the equivalent width of the Li I feature of 4–12 mÅ derived from the synthetic fits (see Table 1) are consistent with our estimate of the statistical errors in the spectra.

The Li I doublet was detected in the star III-57 which is at the base of the red giant branch. A second spectrum of higher resolution and higher S/N was acquired in 1994 January at the 4 m KPNO telescope to confirm our detection. That spectrum is shown together with synthetic fits with log ϵ(Li) = 0.5 and 0.85 in Figure 1*a*; log ϵ(Li) = 0.5 is the measured upper limit in II-22 and IV-77 (Fig. 1*b*) which are at the same evolutionary phase as III-57. It is clear that the observed Li I + Fe I feature is stronger in III-57 than the upper limit measured in IV-77. The Li abundances measured in our spectra of III-57 are log ϵ(Li) = 1.0 and 0.85, which correspond to Li I equivalent widths of 25 and 20 mÅ.

In a previous study, García López, Rebolo, & Beckman (1988) claimed a Li I detection in F135 and derived an abundance of log ϵ(Li) = 0.75. In Figure 1*c* synthetic spectra with log ϵ(Li) = 0.75 and 0.0 are shown together with our observed spectrum of F135. Our higher resolution, higher S/N spectrum shows no evidence for a Li I feature, and our upper limit of log ϵ(Li) < 0.0 is consistent with other giants at the same evolutionary phase.

According to the study of Mathieu et al. (1986) and their continued radial velocity monitoring (D. W. Latham 1993, private communication), none of the stars in our study are members of double-lined binaries. F111, F105, and F170 are single-lined binary systems. Mathieu, Latham, & Griffin (1990) cite the single-lined spectrum as evidence that the companion is at least 2 mag fainter than F111. Our spectra are hence assumed to be uncontaminated by the presence of the secondary, and the syntheses were carried out as for a single star. F117 is listed as a double-lined binary in Mathieu et al. (1986). Our earlier study (Balachandran 1990b) erroneously treated its spectrum as single-lined and reported a lithium measurement of log ϵ(Li) = 1.20. This star will be discussed in a later paper together with a larger sample of double-lined binaries.

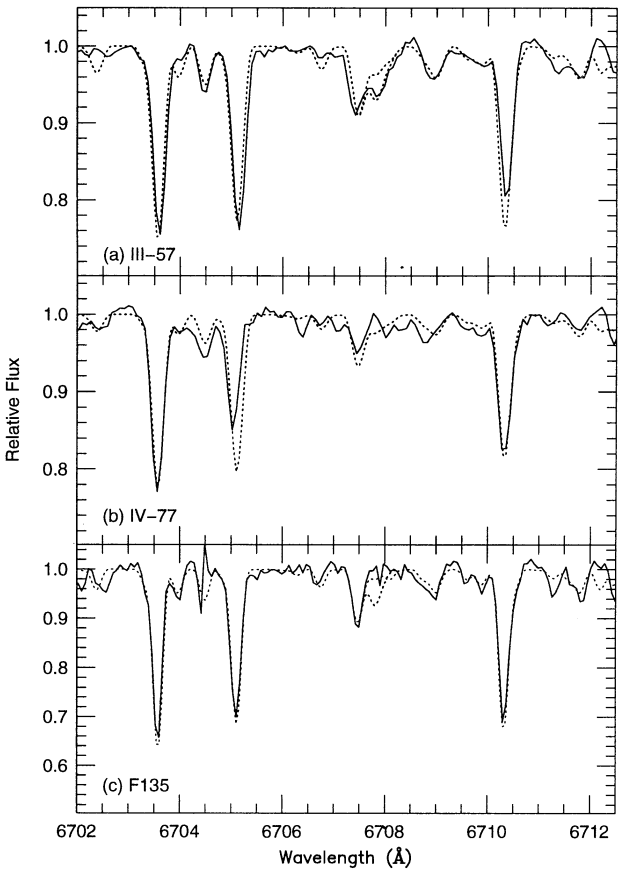

FIG. 1.—Observed spectra are shown as solid lines and synthetic spectral fits as dotted lines for three subgiants and giants in M67: (*a*) III-57 with log ϵ(Li) = 0.5 and 0.85, (*b*) IV-77 with log ϵ(Li) = 0.5, and (*c*) F135 with log ϵ(Li) = 0.0 and 0.75.

3. REANALYSIS OF CLUSTER OBSERVATIONS

Of the open clusters, the Li dip is best defined in the Hyades (Boesgaard & Tripicco 1986, hereafter BT; Boesgaard & Budge 1988, hereafter BB), NGC 752 (Hobbs & Pilachowski 1986a; Pilachowski & Hobbs 1988), and Praesepe (BB; Soderblom et al. 1993a) clusters. Data on the Coma cluster are available but sparse (Boesgaard 1987a; Soderblom et al. 1990), and the questionable homogeneity of the UMa moving group makes for a less favorable comparison (Soderblom et al. 1993c). In the young α Persei (Balachandran, Lambert, & Stauffer 1988) and Pleiades (Soderblom et al. 1993b) clusters, an incipient Li dip is defined only to the fervent believer.

Two previous studies have compared the Li dips in the Hyades and NGC 752. Hobbs & Pilachowski (1988) found that the Li dip was ~90 K cooler in NGC 752 than in the Hyades but concluded that, within the uncertainties in the temperatures of the individual stars, and the metallicity of NGC 752 (solar metallicity was adopted), this difference was not significant. While their comparison used all of the NGC 752 Li

data, only the original BT Hyades data were available to them for their analysis. Furthermore, their analysis of NGC 752 relied on temperature derived from the very inhomogeneous set of photometry then available. This situation has been remedied recently by the detailed study of NGC 752 (Daniel et al. 1994) in which all of the available photoelectric and photometric photometry has been transformed to a uniform standard system. Daniel et al. (1994) performed the second comparison of the Li dips in the Hyades and NGC 752 clusters, but there are several uncertainties in their analysis. While they utilized their standardized photometry for NGC 752 in their comparison, they retained the original Li abundances of Hobbs & Pilachowski (1986a) and Pilachowski & Hobbs (1988). As will be shown later (§ 3.2), changes in the colors of individual stars result in significant changes in their temperatures and Li abundances, and finally in the shape of the Li dip. In addition, they used the mean Hyades Li curve from BT for their comparison and not the actual data from either BT or the more extensive compliation of BB. Most important, since their comparison was carried out in the Li versus $B-V$ plane, and the $B-V$ color is metallicity dependent, the colors of NGC 752 were corrected to the metallicity of the Hyades using the SH effective temperature calibration. The Hyades Li abundances in BT and BB were, however, derived using temperatures based on the Cayrel, Cayrel de Strobel, & Campbell (1985, hereafter C^3) temperature scale, and again, this will be shown later (§ 3.3) to significantly affect the shape of the Li dip and thus any comparison with NGC 752. Daniel et al. (1994) concluded that the shift in the Li dip seen in NGC 752 was merely a result of evolution off the zero-age main sequence (ZAMS), but the shortcomings in their analysis make it necessary to reexamine the clusters with greater care.

3.1. *Temperature Calibration*

Of crucial importance in the comparison of the four clusters is the use of a consistent and well-understood temperature calibration. The Hyades abundances, both in the early to mid-F stars in BT and BB, and in the late-F and G dwarfs in Thorburn et al. (1993), were derived using the temperature scale recommended by C^3 for the Hyades. While retaining the slope of the Carney (1983) $V-K$ calibration, C^3 justified a shift in zero point on the basis of fits to the wings of the Hα profile in solar-type stars. Carney's scale relies upon a comparison of the slope of the flux in the Paschen continuum, generated using Kurucz (1979) model atmospheres, to spectrophotometric scans of 87 stars. His temperature calibration was established by relating the derived temperatures of the stars to their $V-K$ colors and is stated to be valid for $V-K = 0.9$–2.2 ($T_{\rm eff}$ = 7000–4500 K). A recent reexamination of this temperature scale using newly available photometry has resulted in a slight revision in the slope and zero point of the calibration and the introduction of a small metallicity dependence (Carney et al. 1994; see Fig. 2). The C^3 zero-point shift was obtained by comparing synthetic Hα profiles to the spectra of seven Hyades dwarfs which bracket the solar temperature by roughly ± 150 K. C^3 stated that their relationship was valid for the entire temperature range covered by Carney (1983), but their calibration was tested spectroscopically only for stars between 5000 and 6000 K, and in this temperature range they found [Fe/H] to be independent of temperature. Figure 2 compares the various calibrations for the metallicity of the Hyades. $V-K$ colors have been transformed to $B-V$ colors using Carney's (1983) relationship for the Hyades.

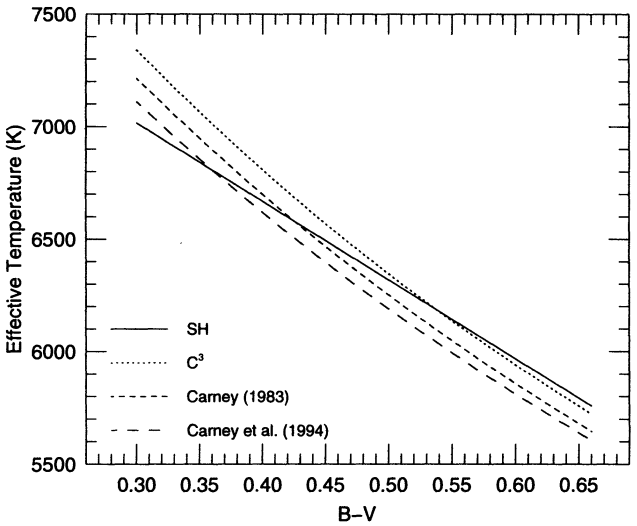

FIG. 2.—Effective temperature calibrations of Carney et al. (1994, *long-dashed line*), Carney (1983, *short-dashed line*), C^3 (*dotted line*), and SH (*solid line*) are compared for [Fe/H] = 0.12, the metallicity of the Hyades.

An independent temperature calibration for F dwarfs based on the infrared flux method of Blackwell & Shallis (1977) was derived by SH. Since the SH calibration is in terms of $B-V$ colors, which is the most comprehensive set of colors available for all four clusters under consideration, and since their calibration has an explicit metallicity-dependent term, it makes for a very useful calibration in the present context. While SH agrees with C^3 at solar temperatures, there is a large difference of nearly 400 K at 7000 K (Fig. 2). *Use of the C^3 scale hence results in a much wider Li dip in the Hyades relative to SH scale.* The empirically determined effective temperatures of the Sun and Procyon provide independent checks of the two calibrations. SH obtained a good fit to the measured solar angular diameter. The solar temperature will hence be taken to be secure in both the SH and C^3 calibrations, though the uncertain value of the solar $B-V$ color remains a source of possible error. SH also obtained a good fit to the measured angular diameter of Procyon. Using $B-V = 0.42$ and solar metallicity for Procyon, their calibration yields an effective temperature of 6555 K, in good agreement with the Code et al. (1976) empirical determination of 6510 ± 130 K. Using $V-K_{\rm CIT} = 1.0$ for Procyon, C^3 yields $T_{\rm eff} = 6746$ K, much larger than the empirical determintion within the errors. Thus, the C^3 calibration overestimates the temperature at 6600 K, and since the difference between the two calibrations continues to increase at higher temperatures, extrapolation of the C^3 calibration to 7000 K must be held suspect.

Commenting upon the high [Fe/H] abundances in their hotter Hyades F dwarfs, BB suggested that the C^3 calibration may yield anomalously high temperatures. The BT, BB, and more recent Boesgaard (1989) studied provide the necessary Fe I data for a spectroscopic check on the C^3 and SH temperature calibrations. For the six Fe I lines measured in these studies, solar *gf*-values were derived using equivalent widths measured from the digital version of the solar flux atlas (Kurucz et al. 1984) and the solar atmosphere from the Kurucz (1979) grid with $12 + (\mathrm{Fe/H})_\odot = 7.50$ (Holweger et al. 1991; Biémont et al. 1991) (see Table 2). Temperatures were estimated using both the C^3 and SH calibrations, the latter with [Fe/H] = +0.12 (C^3). Note that since the metallicity derived by C^3 rests on solar-type stars, it is not affected by possible temperature discrepancies in the hotter stars. Equivalent

TABLE 2

Fe I Line Parameters

Wavelength (Å)	EP[a] (eV)	log *gf*	Solar EW (mÅ)
6677.997.....	2.690	−1.350	135
6703.580.....	2.760	−3.050	38
6705.105.....	4.610	−1.048	47
6726.670.....	4.610	−1.009	49
6750.160.....	2.420	−2.614	73
6752.716.....	4.640	−1.186	39

[a] EP = excitation potential.

widths listed as uncertain were discarded, where more than one measurement for the same star is listed, the most recent value was preferred. Temperatures and [Fe/H] abundances based on both calibrations are listed in Table 3. Our abundances based on the C^3 calibration are in reasonable agreement with the values derived by BT, BB, and Boesgaard (1989).

In Figure 3, the two sets of abundances are plotted as a function of the adopted temperatures together with a linear least-squares fit to the data. While the C^3 calibration overestimates the effective temperatures of the hot stars, SH appears to underestimate them. The magnitude of the SH slope is smaller than the C^3 slope, indicating that it is a better temperature estimator. There are, unfortunately, only three Hyades stars with $T_{\rm eff} > 6700$ K (according to the SH calibration), and their abundances are crucial to the SH fit. In the absence of these three stars, the slope of the SH fit is smaller in magnitude by a factor of 2, while the deletion of the same three stars produces virtually no change to the C^3 fit. A larger set of high-S/N spectra of early-F stars in the Hyades would be invaluable to constrain the temperature calibrations.

TABLE 3

Comparison of C^3 and SH Temperature Calibrations

	C^3 Calibration		SH Calibration		
van Bueren	$T_{\rm eff}$ (K)	[Fe/H]	$T_{\rm eff}$ (K)	[Fe/H]	EW Source[a]
6.....	7110	0.18	6875	0.06	BB
8.....	6710	0.25	6603	0.18	BB
11.....	6850	0.10	6683	0.01	B
13.....	6725	0.24	6600	0.18	BT
14.....	7042	0.19	6826	0.07	BT
19.....	6300	0.19	6279	0.19	B
20.....	6860	0.30	6673	0.17	BB
36.....	6613	0.34	6526	0.28	BT
37.....	6814	0.25	6652	0.18	BT
38.....	7376	0.32	6949	0.05	BT
44.....	6563	0.13	6495	0.06	B
48.....	6246	0.04	6247	0.04	B
51.....	6596	0.15	6519	0.12	B
59.....	6120	0.12	6171	0.19	B
61.....	6260	0.15	6272	0.15	B
62.....	6185	0.12	6192	0.12	BB
65.....	6200	0.10	6198	0.10	B
77.....	6330	0.07	6317	0.07	BB
78.....	6510	0.11	6485	0.11	B
81.....	6471	0.14	6425	0.09	B
85.....	6680	0.02	6579	−0.03	BB
86.....	6484	0.05	6450	0.05	B
90.....	6740	0.10	6624	0.05	BB
94.....	6651	0.08	6561	0.08	BT
101.....	6635	0.17	6554	0.17	BB
121.....	6337	0.16	6307	0.16	B
128.....	6562	0.13	6495	0.07	B

[a] Fe I equivalent widths were taken from: BT = Boesgaard & Tripicco 1986; BB = Boesgaard & Budge 1988; B = Boesgaard 1989.

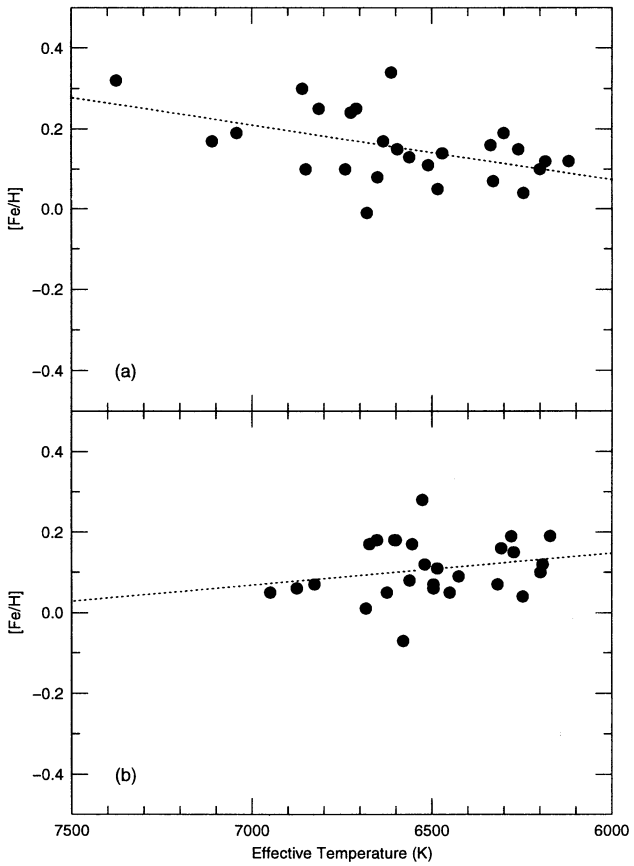

Fig. 3.—[Fe/H] derived using the temperature calibrations of (*a*) C^3 and (*b*) SH are plotted as a function of $T_{\rm eff}$ for Hyades stars. The equivalent width data for the Fe I lines used in the analysis were taken from BT, and Bosegaard (1989). The dotted lines are linear least-squares fits to the abundances.

Since we propose to look for differences due to metallicity in the Li dips of the four clusters, we require that the metallicity-dependent term in the temperature calibration be well understood. The *uvbyHβ* calibration of Edvardsson et al. (1993, hereafter EAGLNT) based on model atmospheres provides an independent check on the SH calibration. Both calibrations are compared in Figure 5*a* of EAGLNT. Note that the comparison is based on the $b-y$ calibration of SH, but since the same data were used to derive their $B-V$ calibration, any comparison of the former should be valid for the latter as well. There is good agreement between the EAGLNT and SH calibrations at solar temperature and metallicity. At higher temperatures, the steeper EAGLNT calibration predicts larger values than SH. Again, Procyon provides a useful check. EAGLNT predicts $T_{\rm eff} = 6704$ K, somewhat higher than the empirical value of Code et al. (1976). Thus, SH remains a better predictor of temperatures around 6600 K. We note that while EAGLNT have found that their spectroscopically determined metallicities agree well with their photometric calibration, their sample is sparse at temperatures hotter than 6600 K (see their Fig. 9). Thus the high end of the EAGLNT temperature calibration remains untested and the need for additional high-S/N data is reiterated. Differences in temperature due to differences in metallicity can be compared at a given color. Figure 5*a* of

EAGLNT shows effective temperature as a function of $b-y$ for [Fe/H] = +0.3, 0.0, and −0.5. Interpolating linearly in metallicity, at $b-y = 0.27$ ($T_{\rm eff} \sim 6600$ K), a metallicity difference of 0.3 dex (which corresponds roughly to the metallicity difference between the Hyades and NGC 752) results in a temperature difference of 92 K according to the EAGLNT calibration. At the same temperature ($B-V \approx 0.4$), the SH calibration, in excellent agreement, gives a temperature difference of 85 K for the same range in metallicity. At cooler temperatures, the difference between the two calibrations is slightly larger. At $b-y = 0.33$, which corresponds roughly to $T_{\rm eff} = 6250$ K, EAGLNT yields a difference of 79 K for a metallicity difference of 0.3 dex, while SH yields a difference of 107 K at the same temperature ($B-V \sim 0.51$). Thus the metallicity dependence in the SH calibration is in reasonable agreement with the independent derivation of EAGLNT.

After this detailed examination, the SH calibration was adopted for our cluster analysis. For the purpose of comparison with theoretical models, we note that SH probably produces a narrower dip than is "correct" by underestimating temperatures of the hotter stars. However, we conclude that the Hyades dip is better defined by the SH scale than by the C^3 scale. For the metallicity range in our clusters, the SH calibration will yield the same differences in temperature with metallicity as the independent $b-y$ calibration of EAGLNT.

It is useful to examine whether improvements in the input physics made since the derivation of the SH calibration have a significant effect on it. The SH calibrations used the MARCS opacities of Gustafsson et al. (1975) to compute the monochromatic surface fluxes required in the infrared flux method of Blackwell & Shallis (1977). Blackwell & Lynas-Gray (1994) have recently recomputed temperatures and angular diameters with the new Kurucz (1990) grid of heavily blanketed model atmospheres for the same sample of stars for which temperatures had earlier been derived using MARCS opacities (Blackwell et al. 1990). Comparison of the two sets of temperatures shows that the improved Kurucz grid has only a small effect on temperatures in the range of the SH calibration. The new temperatures are ∼50 K hotter at 58000 K, 30 K cooler at 7000 K, and identical to the old values at the temperature of the Li dip. Blackwell, Lynas-Gray, & Petford (1991) have studied the temperature effects due to improved H^- opacities in the MARCS models and found them to be negligible for stars hotter than 6000 K.

The Böhm-Vitense (1981) calibration is adopted for stars outside the range of the SH calibration ($B-V > 0.63$). The Böhm-Vitense (1981) calibration does not distinguish in temperature between stars of the same color but different metallicity, and hence there is no information in our analysis on abundance variations with metallicity in stars cooler than 5800 K. There is a difference of ∼200 K between the SH and Böhm-Vitense calibrations at 7000 K. SH suggest that this may result from errors in the Böhm-Vitense calibration. However, the two calibrations agree well at the cool end of the SH scale, and thus we expect a smooth change in our stellar temperature estimates at the transition between the two calibrations. It should be noted that the error in the Böhm-Vitense calibration is larger (±200 K), while SH claim a much smaller zero-point error of ±75 K. While stars redder than $B-V = 0.63$ are well outside the range of the Li dip and play no part in our discussion of the dip morphology, they are important in cluster comparisons (see § 4) and add significant insight into our understanding of Li depletion.

3.2. *Masses and ZAMS Temperatures*

The temperatures of the dip stars in the younger Hyades and Praesepe clusters are not very different from their ZAMS temperatures (see §§ 3.3 and 3.4). However, the dip stars in the older NGC 752 cluster are near the cluster turn-off, and those in M67 have evolved off the main sequence, resulting in their present temperatures being different from their ZAMS temperatures. Therefore, the morphology of the Li dips in the Hyades and Praesepe can only be compared with those in NGC 752 and M67 if the masses and ZAMS temperatures of the individual stars are derived using theoretical isochrones. The grid of Revised Yale Isochrones (Green, Demarque, & King 1987, hereafter RYI) was chosen for this purpose because isochrones of the appropriate metallicity can be easily interpolated for each cluster. While the derived masses and ZAMS temperatures may show systematic variations if a different set of theoretical isochrones is utilized, the relative differences we seek to understand in the Li dip morphologies should remain essentially the same. In their examination of the ages of old disk clusters, including M67, Demarque et al. (1992) have discussed in detail the effects of different opacity grids and surface boundary conditions and concluded that as long as the proper solar calibration is applied, the derived age of the cluster remains unchanged.

The RYI grid is calibrated to the Pleiades and Praesepe clusters. Demarque et al. (1992) find that this calibration used to set the zero point in the RYI grid results in a 1 $M_\odot$ star having a temperature 100 K cooler than the Sun at 4.5 Gyr. In order to get the same age for M67 as via solar calibrated isochrones, they adopted a reddening value of $E(B-V) = 0.06$, which is slightly larger than the recommended value of $E(B-V) = 0.04$ (Nissen et al. 1987). We have chosen to simply shift all of the RYI tracks to hotter temperatures by 100 K. This permits us to use the best reddening estimated for each cluster and thus our Li abundances remain unaffected by systematic shifts in the temperature. Our shift in the temperatures of the isochrones simply results in a slight systematic decrease in all of the masses we derive, but does not affect the cluster comparisons. For each cluster, the isochrone of the appropriate age and metallicity was interpolated from the RYI grid and used to determine the mass of the each star in that cluster from its effective temperature. The derived masses and the ZAMS isochrone of the same metallicity were then used to determine ZAMS temperatures.

3.3. *The Hyades*

The Hyades stars examined here are from BT, BB, and Thorburn et al. (1993). Soderblom et al. (1990) have also examined Li abundances in Hyades G dwarfs, but since their smaller sample is almost fully contained in Thorburn et al., the latter was preferred. A sample of Hyades A stars has been analyzed for Li by Burkhart & Coupry (1989, 1991). Only two of these are cool enough to fall within the SH calibration, and in the interest of maintaining homogeneity, these are not included in our sample. All double-lined binaries identified by Griffin et al. (1988) were excluded from further analysis. The full sample used in our study is identified by the van Bueren (1952) number of the star in Table 4. $B-V$ colors were taken from Johnson & Knuckles (1955) and $E(B-V) = 0.0$ (Cayrel de Strobel 1990) was adopted. Temperatures were derived using the SH calibration with [Fe/H] = 0.12 for $B-V \leq 0.63$ and the Böhm-Vitense (1981) temperature calibration for

TABLE 4

HYADES: TEMPERATURES, Li ABUNDANCES, MASSES, AND ZAMS TEMPERATURES

VAN BUEREN	V	$B-V$	T_{eff}[a] (K)	log ϵ(Li)	MASS ($M_\odot$)	ZAMS T_{eff} (K)	SOURCE[b]
1.....	7.40	0.566	6090	2.97	1.215	6067	T
2.....	7.78	0.617	5912	2.74	1.140	5916	T
4.....	8.88	0.848	5224	<0.56	0.847	5099	T
6.....	5.97	0.341	6875	3.05	1.524	6897	BT
8.....	6.37	0.419	6603	<1.65	1.411	6544	BB
9.....	8.67	0.708	5524	...	0.966	5526	T
10.....	7.85	0.589	6010	2.76	1.182	6000	T
11.....	6.01	0.396	6683	2.31	1.442	6636	BT
13.....	6.62	0.420	6600	<1.76	1.410	6542	BT
14.....	5.73	0.355	6826	3.10	1.502	6825	BT
15.....	8.09	0.658	5682	2.32	1.037	5703	T
17.....	8.46	0.696	5535	1.86	0.971	5539	T
18.....	8.06	0.638	5758	2.42	1.072	5779	T
19.....	7.14	0.512	6279	2.89	1.290	6231	BB
20.....	6.32	0.399	6673	3.21	1.438	6624	BB
21.....	9.15	0.816	5294	...	0.872	5207	T
26.....	8.63	0.743	5454	1.46	0.936	5437	T
27.....	8.46	0.715	5510	1.74	0.960	5509	T
31.....	7.47	0.566	6090	2.87	1.215	6067	T
36.....	6.80	0.441	6526	1.15	1.382	6463	BT
37.....	6.61	0.405	6652	1.92	1.430	6600	BT
38.....	5.72	0.320	6949	2.49	1.560	7019	BT
39.....	7.86	0.678	5614	1.96	1.006	5630	T
40.....	6.99	0.563	6101	3.00	1.220	6077	T
42.....	8.86	0.759	5438	1.26	0.929	5414	T
44.....	7.19	0.450	6495	2.20	1.371	6433	BT
46.....	9.11	0.867	5176	<0.93	0.832	5028	T
48.....	7.14	0.521	6247	2.91	1.278	6203	BT
49.....	8.24	0.585	6024	2.52	1.188	6012	T
51.....	6.97	0.443	6519	1.38	1.380	6457	BT
52.....	7.80	0.597	5982	2.77	1.170	5976	T
59.....	7.49	0.543	6171	2.84	1.248	6136	BB
61.....	7.38	0.514	6272	3.12	1.287	6224	BB
62.....	7.38	0.537	6192	3.20	1.256	6154	T
63.....	8.06	0.632	5782	2.49	1.082	5800	T
64.....	8.12	0.657	5686	2.29	1.039	5707	T
65.....	7.42	0.535	6198	3.02	1.259	6160	BB
66.....	7.51	0.555	6129	2.76	1.231	6100	T
69.....	8.64	0.746	5448	1.15	0.933	5427	T
73.....	7.84	0.609	5940	2.66	1.152	5940	T
76.....	9.20	0.759	5420	1.29	0.922	5392	T
77.....	7.05	0.500	6317	2.29	1.304	6263	BB
78.....	6.92	0.453	6485	2.49	1.367	6422	BB
81.....	7.10	0.470	6425	1.98	1.345	6365	BT
85.....	6.51	0.426	6579	<1.83	1.402	6519	BB
86.....	7.05	0.463	6450	2.23	1.354	6388	BT
87.....	8.58	0.743	5454	1.29	0.936	5437	T
90.....	6.40	0.413	6624	<1.52	1.419	6568	BB
91.....	8.94	0.883	5134	<0.28	0.820	4968	T
92.....	8.66	0.741	5458	1.37	0.938	5443	T
93.....	9.40	0.883	5134	<0.28	0.820	4968	T
94.....	6.62	0.431	6561	<1.35	1.395	6499	BT
96.....	8.51	0.841	5239	0.84	0.852	5122	T
97.....	7.93	0.634	5774	2.64	1.079	5793	T
99.....	9.38	0.851	5217	...	0.845	5090	T
101.....	6.65	0.433	6554	<1.52	1.393	6493	BB
102.....	7.54	0.603	5961	2.77	1.161	5958	T
105.....	7.53	0.575	6059	2.83	1.203	6042	T
106.....	7.96	0.669	5645	2.29	1.020	5664	T
109.....	9.40	0.817	5293	<0.87	0.871	5203	T
113.....	7.26	0.549	6150	2.81	1.240	6119	T
114.....	8.54	0.723	5494	1.75	0.953	5488	T
115.....	9.09	0.843	5235	...	0.851	5117	T
116.....	9.01	0.821	5284	<0.35	0.868	5191	T
118.....	7.74	0.580	6041	2.80	1.195	6026	T
119.....	7.12	0.559	6115	2.73	1.225	6088	T
121.....	7.29	0.504	6307	3.15	1.301	6256	BT
128.....	6.75	0.450	6495	1.98	1.371	6433	BT
142.....	8.32	0.665	5659	2.19	1.027	5680	T
153.....	8.91	0.859	5197	1.10	0.839	5062	T
178.....	9.00	0.837	5249	0.84	0.856	5139	T
180.....	9.10	0.853	5212	0.78	0.843	5081	T
182.....	8.93	0.844	5233	0.89	0.850	5113	T

[a] Effective temperatures were derived using the SH calibration for stars with $B-V \leq 0.63$ and the Böhm-Vitense 1981 calibration for stars with $B-V > 0.63$.

[b] Source of Li I equivalent widths used in the abundance determination. BT = Boesgaard & Tripicco 1986; BB = Boesgaard & Budge 1988; T = Thorburn et al. 1993.

$B-V > 0.63$. While previous studies have used the Kurucz (1979) grid of model atmospheres, we have chosen to use the Bell et al. (1990) grid so as to be consistent with the atmospheres used for the M67 giants. A comparison shows that for the same equivalent width, Kurucz (1979) models give Li abundances large by 0.05 dex at 7000 K and smaller by 0.02 dex at 5500 K relative to the Bell et al. (1990) models. The equivalent widths reported in BT and BB are taken to be the blend of the Fe I λ6707.4 feature and the Li I doublet, except in cases where only upper limits are reported, in which case the equivalent width is conservatively taken to represent that of Li I alone, as analyzed in BB. The Thorburn et al. (1993) study lists both blended and deblended Li I equivalent widths; the latter were derived by fitting the observed spectral feature with two components at the Fe I and Li I wavelengths. At the cool end of the Thorburn et al. sample (5500–5000 K), the CN contribution to the spectral feature equals the Li I contribution at 3–4 mÅ, but this has been disregarded in their analysis. We have preferred to match their blended (Li I + Fe I + CN) equivalent width with a synthetic equivalent width derived by using the appropriate model atmosphere from the Bell et al. (1990) grid. The synthetic equivalent width contains contributions from all of the blends, has [Fe/H] = 0.12, and is matched by varying the input Li abundance. The derived Li abundances are listed in Table 4. For three stars (vB 9, 21, and 99), the published equivalent width blend equals the contribution we derive from Fe I and CN alone, and so we do not list a Li abundance in Table 4 for these stars.

Differences in effective temperature dominate the difference between our Li abundances and those in BT and BB. For stars cooler than 6500 K, where the temperature difference is small, our Li abundances agree reasonably well with theirs. Since the C^3 and SH scales are closely matched for the solar-type stars which form the bulk of the hotter stars in the Thorburn et al. (1993) study, temperature differences are at most ± 50 K. We were hence surprised to see relative Li abundance differences as large as 0.3 dex between their abundances and ours. The primary cause of these abundances differences has been traced to the Thorburn et al. usage of the Li I doublet as a single line with *gf*-value equal to the sum of the *gf*- values of the doublet. While this results in only a small abundance overestimate in stars with modest Li equivalent widths, the error increases with increasing equivalent width as the line becomes saturated. The reader is referred to § 3.1 in Balachandran (1988) for a more detailed discussion of this aspect. To demonstrate this trend, Figure 4 plots the difference between the Li abundances derived here and those in Thorburn et al. as a function of their equivalent width measurements. At small equivalent widths, our analysis produces a systematically larger abundance of $\sim$0.06 dex with respect to Thorburn et al. Relative to this zero-point offset, the largest equivalent width measurement (in vB 62) results in a Li abundance overestimate of 0.24 dex in Thorburn et al. We note that both BB and Thorburn et al. have observed vB 62, and while both report nearly identical equivalent width measurements of W_λ (Fe I + Li I) = 131 and 132 mÅ, respectively, the abundances listed by the two studies vary widely: log ϵ(Li) = 3.03 in BB and log ϵ(Li) = 3.36 in Thorburn et al. Our analysis confirms that the abundances derived from the Li I feature in vB 62 when treated as a single line with $gf = 1.483$ and as a doublet with *gf*-values of 0.989 and 0.494 differ by 0.3 dex, with the single line yielding the larger value.

The anomalously large Li abundance in vB 62 was singled out for comment in Thorburn et al. because it is a short-period, tidally locked binary in which any Li overabundance may be linked to its rotational history and the absence of spin-down once this system is tidally synchronized (Pinsonneault, Kawaler, & Demarque 1990), and may provide a clue to the process of Li depletion in general. Their observation that the Li abundance in vB 62 exceeded the value measured in early-F stars on the hot side of the Li dip (Fig. 5*a*) led Thorburn et al. to conjecture that vB 62 was "peculiar" in either having formed with an unusually high Li abundance, or in having retained all of its Li due to its unique rotational history implying that other early-F stars must have undergone a modest amount of depletion. The latter would indicate that the Li abundance of vB 62 reflects the initial abundance with which all Hyades stars formed. In an earlier study, Soderblom et al. (1990) had also found an unusually high abundance in vB 62 and similarly commented upon its binarity as being the possible cause. Since Soderblom et al. (1990) obtain a smaller equivalent width W_λ(Li) = 117 mÅ, their large Li abundance is probably due to their higher temperature of 6460 K; a more detailed discussion of their temperature scale and abundance determination will not be carried out here. According to our analysis, while vB 62 remains the star with the largest Li abundance among other Hyads of its temperature, it is only 0.08 dex higher than vB 61, a normal single star at the same temperature, and is at the same abundance level as stars on the hot side of the Li dip (see Fig. 5*b*). Thus, if the Li abundance in vB 62 has been affected by its rotational history, the effect is small in this star with a moderately long rotational period of 8.55 days (Griffin & Gunn 1978), and vB 62 and the early-F stars in the Hyades are compatible with having originated from interstellar medium (ISM) gas which had the meteoritic Li abundance of log ϵ(Li) = 3.3. As a result of our reanalysis, the Li spread in stars between 6000 and 6300 K observed by Thorburn et al. (1993) decreases by 0.16 dex, but remains real and significant.

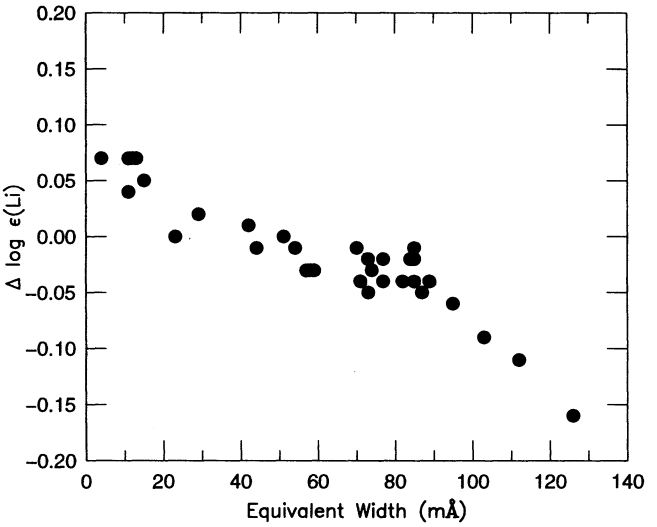

FIG. 4.—Difference between the Li abundances derived in this work and those listed in Thorburn et al. (1993) for the Hyades are plotted as a function of the Li I equivalent width. Temperatures and equivalent widths used are those listed in Thornburn et al., and the abundance difference is due only to the usage of the Li I feature as a single line by Thorburn et al. and as doublet by us.

Figure 5 compares the dip in the Hyades as derived from the C^3 temperature scale with that from the SH calibration. The SH calibration alters the shape and position of both the hot

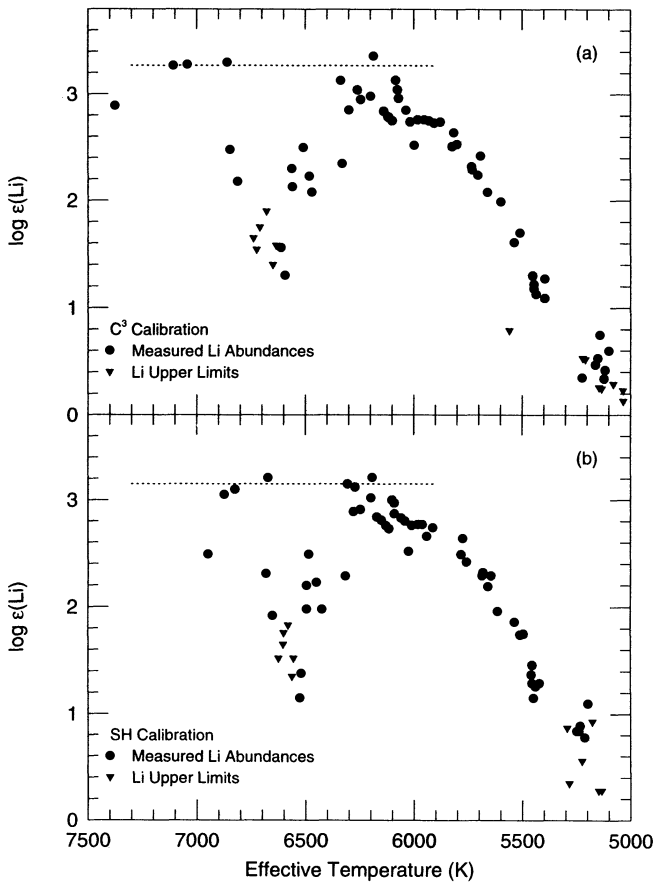

FIG. 5.—Hyades Li dip as a function of $T_{\rm eff}$ using (*a*) the C^3 temperature calibration and Li abundances listed in BT, BB, and Thorburn et al. (1993) and (*b*) the SH calibration with Li abundances rederived in this work. Filled circles are measured Li abundances, and triangles are upper limits. In both plots, the dotted line represents the mean Li abundance of the three stars *hotter* than the Li dip.

and cool sides of the dip, but the effect of the hot side is larger, with the SH dip being considerably narrower and steeper than C^3. The Li dip is centered at $\sim$6550 K in the SH calibration, compared to 6700 K in the C^3 calibration, and the sharp drop in Li on the hot side of the dip makes the shape of the SH dip highly asymmetric. It is also instructive to note that the SH calibration results in equalizing the upper Li abundance envelope on the hot and cool sides of the Hyades Li dip. For our purpose, we define the upper envelope as the average of the three stars with the largest Li abundances. According to the C^3 calibration, the upper envelope is at log ϵ(Li) = 3.28 $\pm$ 0.02 on the hot side of the dip, which is larger than log ϵ(Li) = 3.16 $\pm$ 0.04 on the cool side. Note that equivalent widths and not abundances were used from the Thorburn et al. study in order to derive the abundances on the cool side. The SH calibration yields an upper envelope at log ϵ(Li) = 3.11 $\pm$ 0.09 on the hot side of the dip consistent with log ϵ(Li) = 3.16 $\pm$ 0.04 on the cool side. This result is illustrated graphically in Figures 5*a* and 5*b* in which the dotted lines show the upper envelope as derived from the hot side of the dip.

Recall that for the sake of simplicity, our analysis has assumed a negligible contribution by ^{6}Li. Using the best available ISM estimate for the ^{6}Li/^{7}Li ratio of 0.08 (Lemoine et al. 1993), and assuming that the hot F stars which inhabit the upper Li envelope have not undergone any Li depletion, the ^{7}Li abundance is lowered to log ϵ(Li) = 3.11. Within the uncertainty in the absolute temperatures of these stars and differences introduced by the various grids of model atmospheres, this value is compatible with the meteoritic determination of log ϵ(Li) = 3.3 on an absolute scale.

In order to derive masses and ZAMS temperatures, the age of the Hyades cluster was taken to be 750 Myr (Cayrel de Strobel 1990) and its distance modulus $m-M$ = 3.4 (Schwan 1991). The isochrone of this age and [Fe/H] = 0.12 (C^3; Boesgaard 1989) was interpolated from the RYI grid and is plotted together with the stars in our sample in Figure 6. Recall that the metallicity estimates have been made from solar-type stars whose temperatures derived from the C^3 and SH calibrations are in agreement. Masses were determined from this isochrone using the effective temperature of the star, and ZAMS temperatures were obtained from the derived masses and a ZAMS isochrone of the same metallicity (Table 4). Since the Hyades stars have not evolved far off the ZAMS, the differences between the current and ZAMS temperatures are small. Also becase of the youth of the cluster, the F and G dwarfs being examined are well removed from the cluster turn-off, so that errors in the age estimate of the cluster will result in insignificant errors in the derived masses and ZAMS temperatures.

3.4. *Praesepe Cluster*

Praesepe is of particular interest because it is the same age as the Hyades, and any Li abundance differences between these two clusters must be due to variations in other parameters. Our curiosity about this cluster was piqued by the Soderblom et al. (1993a) study which revealed no variations in Li between the Hyades and Praesepe F stars but significant differences in the G stars, with Praesepe showing larger abundances (see their Fig. 4). It seemed conceivable to us that once the F stars were calibrated in the same way as the Hyades, differences may be seen in these as well.

The Praesepe sample gathered from Soderblom et al. (1993a) and BB is listed in Table 5 by the Klein-Wassink (1927)

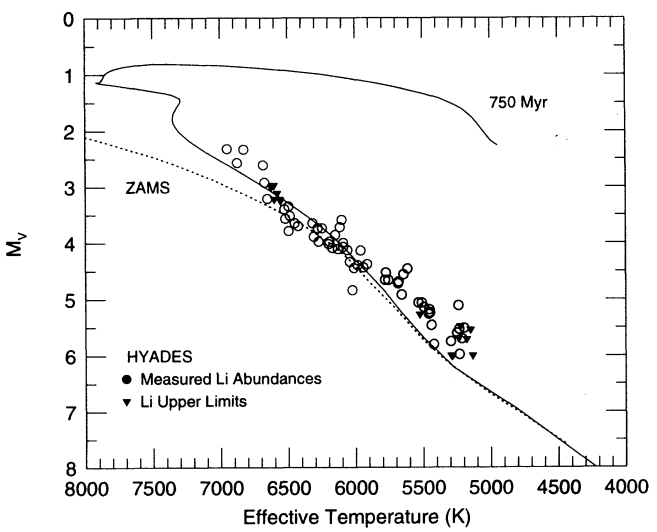

FIG. 6.—H-R diagram showing the Hyades stars used in our study together with the 750 Myr and ZAMS isochrones for [Fe/H] = +0.12 interpolated from the RYI grid. Circles are measured Li abundances, and triangles are Li upper limits.

TABLE 5

PRAESEPE: TEMPERATURES, Li ABUNDANCES, MASSES, AND ZAMS TEMPERATURES

KLEIN-WASSINK	V	$B-V$	$T_{\rm eff}$[a] (K)	log ϵ(Li)	MASS ($M_\odot$)	ZAMS $T_{\rm eff}$ (K)
23	11.29	0.710	5520	1.62	0.939	5560
27	11.44	0.730	5480	<1.22	0.924	5517
30[b]	11.40	0.730	5480	1.92	0.924	5517
32	11.65	0.780	5374	<1.10	0.887	5397
34	9.50	0.430	6538	<2.36	1.332	6471
47[c]	9.87	0.480	6360	<1.82	1.263	6285
49	10.66	0.580	6005	3.03	1.124	5976
58	11.26	0.680	5608	2.04	0.971	5645
70	11.31	0.790	5352	<1.10	0.880	5372
90	10.90	0.700	5540	1.94	0.946	5580
100	10.55	0.580	6005	2.47	1.124	5976
127[c]	10.80	0.610	5898	2.83	1.082	5891
162	10.53	0.570	6040	2.69	1.137	6002
164	11.31	0.710	5520	1.89	0.939	5560
181[c]	10.47	0.610	5898	2.40	1.082	5891
196	10.74	0.590	5969	2.62	1.109	5945
208	10.66	0.590	5969	2.77	1.109	5945
217	10.23	0.500	6289	2.79	1.236	6219
218	9.40	0.420	6573	<2.11	1.345	6509
222	10.11	0.480	6360	2.71	1.263	6285
227[d]	9.49	0.414	6594	1.99	1.353	6533
238[c]	10.30	0.510	6254	2.65	1.222	6186
239	9.67	0.430	6538	<2.08	1.332	6471
250[d]	9.79	0.466	6410	2.07	1.283	6336
258	10.25	0.570	6040	2.30	1.137	6002
288	10.69	0.580	6005	2.71	1.124	5976
293	9.89	0.480	6360	2.49	1.263	6285
295[d]	9.37	0.416	6587	2.53	1.351	6527
301	11.17	0.660	5676	2.31	0.996	5706
304	11.52	0.750	5440	1.31	0.910	5473
322[c]	10.87	0.680	5608	2.21	0.971	5645
325[c]	10.61	0.600	5934	2.59	1.096	5919
326[c]	11.34	0.720	5500	1.64	0.931	5537
332[d]	9.55	0.434	6523	<2.04	1.326	6454
334	11.02	0.710	5520	1.73	0.939	5560
335	11.03	0.630	5827	2.51	1.054	5833
336	11.46	0.710	5520	1.58	0.939	5560
341	10.30	0.520	6218	2.90	1.208	6154
368[c]	11.52	0.720	5500	1.87	0.931	5537
370	9.04	0.340	6857	2.92	1.449	6844
371	10.11	0.500	6289	2.70	1.236	6219
392	10.72	0.600	5934	1.57	1.096	5919
396	9.88	0.470	6396	2.43	1.278	6323
399	10.93	0.620	5863	2.59	1.068	5862
416[d]	9.59	0.412	6602	3.12	1.356	6542
418	10.47	0.570	6040	2.85	1.137	6002
421	10.17	0.520	6218	3.06	1.208	6154
432[c]	11.05	0.640	5750	2.41	1.024	5769
434[c]	11.41	0.720	5500	<1.17	0.931	5537
439[c]	9.48	0.400	6644	2.99	1.372	6591
454	9.88	0.470	6396	2.55	1.278	6323
466	10.99	0.650	5710	2.41	1.009	5736
476	11.62	0.760	5418	1.59	0.902	5448
488	11.44	0.730	5480	1.84	0.924	5517
498	11.78	0.780	5374	<1.10	0.887	5397
508[c]	10.77	0.590	5969	2.81	1.109	5945
540	11.03	0.690	5574	2.49	0.958	5612
541[b]	10.66	0.630	5827	2.55	1.054	5833
549[c]	10.13	0.480	6360	3.32	1.263	6285

[a] Effective temperatures were derived using the SH calibration for stars with $B-V \leq 0.63$ and the Böhm-Vitense 1981 calibration for stars with $B-V > 0.63$.

[b] Temperatures derived from $V-I$ colors are hotter than those derived from $B-V$ colors.

[c] Stars listed as SB in Soderblom et al. 1993a.

[d] Li I equivalent widths for these stars have been taken from Boesgaard & Budge 1988. Equivalent widths for the remaining stars are from Soderblom et al. 1993a.

number. All of the double-lined and photometric binaries listed in Soderblom et al. were discarded. $B-V$ colors were taken from Johnson (1952) and Mendoza (1967). The reddening of $E(B-V) = 0.0$ (Cayrel de Strobel 1990) and metallicity [Fe/H] = 0.04 (Friel & Boesgaard 1992) were adopted. The temperatures of the six stars utilized by Friel & Boesgaard (1992) for their metallicity determination agree with the SH calibration temperatures to within ± 100 K. Soderblom et al. (1993a), assuming the Hyades metallicity for Praesepe, transformed Mendoza's (1967) $V-I$ colors to $V-K$ colors and derived temperatures via the C^3 Hyades calibration. Preferring $B-V$ colors for their Hyades temperature determination, Thorburn et al. (1993) argued that the presence of an undetected cool companion will result in a greater increase in the $V-I$ than the $B-V$ color, and indeed, the temperatures of a few known single-lined binaries in Praesepe (KW 325 and 432) are much cooler when derived from their $V-I$ colors than their $B-V$ colors. Others like KW 334, 336, and 339, which show a similar trend but are not identified as spectroscopic binaries, may have undetected companions as well. It is puzzling that some stars like KW 30 and 541 produce hotter temperatures from their $V-I$ colors compared to their $B-V$ colors. The $B-V$ colors of Mendoza (1967) agree well with those of Johnson (1952); for 42 stars in common, the mean difference is 0.0005 ± 0.008 dex. However, no independent source of $V-I$ colors is available. We note that Mendoza's (1967) $V-I$ colors show a much larger scatter than $B-V$ colors when plotted versus V, and Mendoza (1967) states that his $V-R$ colors have larger errors than $B-V$. If the larger scatter in the $V-I$ colors arises from photometric errors as well, temperatures derived from these colors will have an added uncertainty. Thus for these two principal reasons the $B-V$ color must be preferred as the more accurate temperature indicator despite its larger metallicity dependence in the cooler G dwarfs. Our temperatures for the full sample of Praesepe stars are listed in Table 5. There is a scatter of ± 200 K between our temperatures and those listed in Soderblom et al. With the exception of KW 416, our temperature calibration produces little change in the BB Praesepe temperatures.

Soderblom et al. have deblended the Fe I and CN contaminant from their observed Li I spectral feature blend by using an empirical relationship based on color (Soderblom et al. 1993b). In order to be consistent with the Hyades analysis, we have added this blend back into their listed equivalent widths and used the synthetic equivalent width matching technique described in § 3.3 to determine the Li abundances (Table 5). Blended equivalent widths are listed in BB, and Li abundances were derived similarly from these (Table 5). For the most part, changes in Li abundances were consistent with the changes in the adopted effective temperatures. Seven stars in the Soderblom et al. study (KW 23, 217, 258, 304, 334, 336, and 341) showed much larger abundance changes than expected. We have since learned (D. R. Soderblom 1994, private communication) that the equivalent widths listed in the Soderblom et al. (1993a) paper are correct, but there are errors in the listed abundances. Our derived abundances are better matched with the revised abundance list supplied by D. R. Soderblom (1994, private communication) with a mean difference of -0.05 dex, and near-identical abundance estimates for the same temperature.

The distance modulus $V-M_V = 6.0$ (Johnson 1957) was adopted for Praesepe. A 750 Myr RYI isochrone with

[Fe/H] = 0.04 was used to determine the masses of the individual stars, and a ZAMS isochrone of the same metallicity was used to obtain the ZAMS temperatures (Table 6). As for the Hyades, any uncertainty in cluster age will not significantly affect the mass and ZAMS temperature determinations of the dip stars.

3.5. NGC 752 *Cluster*

Li I equivalent widths in Hobbs & Pilachowski (1986a) and Pilachowski & Hobbs (1988) form the basis for our reanalysis of NGC 752. With the exception of Heinemann 258 and 264, listed as nonmembers in the recent Daniel et al. (1994) study, the remaining stars are listed in Table 6 by their Heinemann (1926) numbers. The principal improvement in NGC 752 since the comparative study of Hobbs & Pilachowski (1988) is the standardized photometry of Daniel et al. (1994). Our temperatures were derived using these standardized $B-V$ colors (listed in Table 6), $E(B-V) = 0.035$, and [Fe/H] = -0.15, all taken from Daniel et al. (1994). Lithium abundances were then recalculated. The published equivalent widths were taken to be the sum of the blended Li I feature except for the upper limits which were conservatively treated as those of Li I alone. H207 is listed as having a measured equivalent width of 7 mÅ (Hobbs & Pilachowski 1986a). Since, according to our analysis, the equivalent width of the Fe I blend alone would equal this value at the temperature of the star, we treated the measurement as a Li I upper limit. Because the Fe I blend has not been subtracted from the equivalent widths listed in Hobbs & Pilachowski (1986a) and Pilachowski & Hobbs (1988), their treatment of the equivalent width as unblended resulted in systematically higher abundances than ours even in cases where there is no change in temperature. This bias in their abundances was recognized by Hobbs & Pilachowski (1986a).

TABLE 6

NGC 752: TEMPERATURES, Li ABUNDANCES, MASSES, AND ZAMS TEMPERATURES

Heinemann	V	$B-V$	$T_{\rm eff}$[a] (K)	log ϵ(Li)[b]	Mass ($M_\odot$)	ZAMS $T_{\rm eff}$ (K)
10.....	10.12	0.411	6680	2.67	1.512	7463
88.....	11.78	0.482	6420	<1.93	1.202	6334
94.....	13.84	0.760	5490	<0.91	0.848	5467
123.....	11.20	0.396	6730	<2.54	1.429	7115
139.....	11.79	0.455	6520	<2.00	1.237	6447
146.....	13.06	0.690	5693	2.03	0.913	5690
185.....	12.21	0.529	6240	2.43	1.136	6159
189.....	11.30	0.423	6640	2.97	1.291	6600
197.....	11.64	0.440	6570	<2.02	1.252	6508
207.....	13.20	0.670	5720	<1.25	0.923	5715
222.....	10.84	0.388	6760	2.88	1.432	7127
227.....	14.10	0.930	5103	<0.87	0.757	4925
229.....	12.63	0.553	6160	2.68	1.110	6089
235.....	11.47	0.480	6425	<1.40	1.204	6340
237.....	12.31	0.600	5980	2.30	1.032	5941
254.....	10.90	0.373	6820	2.93	1.438	7152
259.....	11.38	0.419	6650	2.27	1.296	6617
265.....	13.26	0.660	5760	1.32	0.939	5753
266.....	11.21	0.424	6630	2.70	1.287	6587
293.....	11.94	0.484	6410	1.99	1.198	6324
302.....	11.49	0.417	6630	<1.76	1.287	6587
304.....	11.89	0.481	6421	<1.40	1.202	6334

[a] Effective temperatures were derived using the SH calibration for stars with $B-V \leq 0.63$ and the Böhm-Vitense 1981 calibration for stars with $B-V > 0.63$.

[b] Equivalent widths used to determine Li abundances have been taken from Hobbs & Pilachowski 1986a and Pilachowski & Hobbs 1988.

Our temperatures differed by as much as +290 K to −210 K from the earlier published values, and these resulted in correspondingly large changes in the Li abundances. Figure 7 compares the old and new Li dips in NGC 752. Temperatures resulting from the standarized photometry (Daniel et al. 1994) and abundances rederived using these temperatures have resulted in a more clearly defined Li dip.

Daniel et al. (1994) find that the best fit to the cluster turn-off obtained with classical (nonovershoot) isochrones is for an age of 1.9 ± 0.2 Gyr. Adopting a distance modulus $V-M_V = 8.25$ from Daniel et al. (1994), the data are plotted on the H-R diagram together with the RYI 2 Gyr and ZAMS isochrones for [Fe/H] = −0.15 (Fig. 8*a*). In Figure 8*b* mass is plotted as a function of effective temperature for the same two isochrones. It is clear that an error in the estimated age of the cluster can significantly change the derived masses of only the four most massive stars in the sample which have evolved significantly off the ZAMS. Masses for the individual stars were derived from their effective temperatures using the 2 Gyr isochrone, and ZAMS temperatures were then obtained from the derived masses using the ZAMS isochrone of the same metallicity (Table 6). *For the four most massive stars*, the error in the mass due to the age uncertainty of ±0.2 Gyr would be roughly ±0.05 $M_\odot$, which leads to errors in ZAMS temperature determinations of ±200 K.

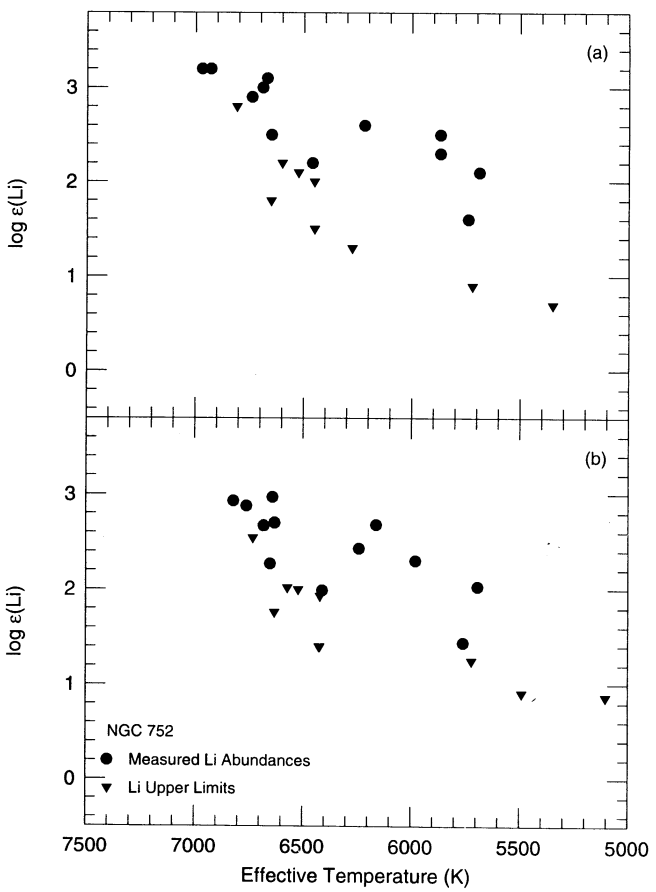

FIG. 7.—NGC 752 Li dip (*a*) as previously published by Hobbs & Pilachowski (1986a) and Pilachowski & Hobbs (1988) and (*b*) as obtained when temperatures were calculated using the standardized photometry of Daniel et al. (1994) and Li abundances were rederived using these temperatures. Filled circles are measured Li abundances, and triangles are upper limits.

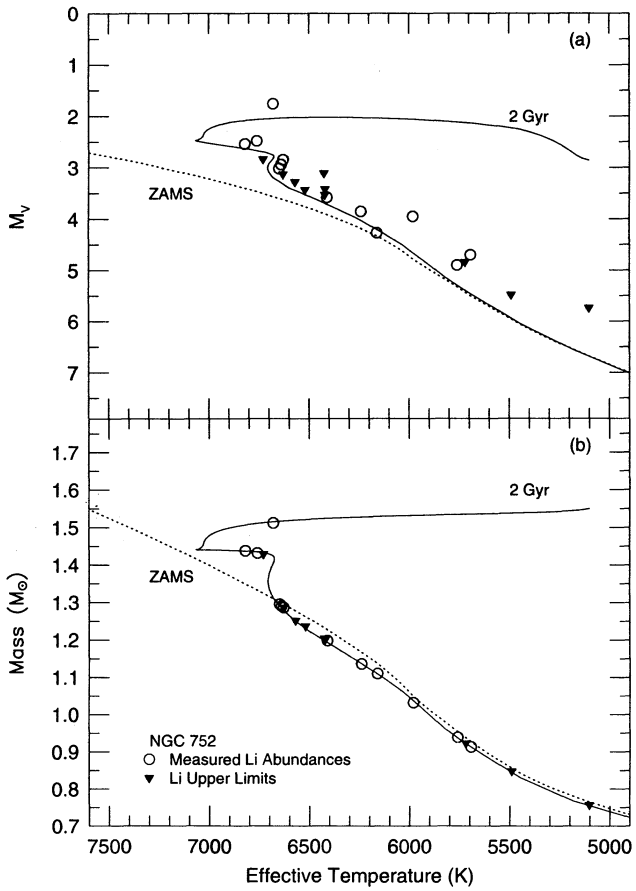

FIG. 8.—(*a*) H-R diagram showing the NGC 752 stars used in this study together with the 2 Gyr and ZAMS isochrones for [Fe/H] = −0.15 interpolated from the RYI grid. (*b*) Masses of the same stars (derived from their $T_{\rm eff}$'s and the 2 Gyr isochrone) are shown as a function of $T_{\rm eff}$ with the same two isochrones. Open circles are measured Li abundances, and filled triangles are Li upper limits.

3.6. *M67 Cluster*

Li data in the turn-off and dwarf stars in M67 have been gathered from Hobbs & Pilachowski (1986b), Spite et al. (1987), and García López et al. (1988). $B-V$ colors were taken from Eggen & Sandage (1964) and effective temperatures derived using $E(B-V) = 0.04$ (Nissen et al. 1987) and solar metallicity (Hobbs & Thorburn 1991; Friel & Bosegaard 1992). Blended Li I equivalent widths are listed in the three studies. These were used to determine Li abundances. Upper limits were treated as Li I alone. The $B-V$ color, temperature, and abundance of each star are listed in Table 7.

According to Demarque et al. (1992), the best fit to M67 is achieved with the 4 Gyr RYI solar metallicity isochrone assuming $E(B-V) = 0.06$ and the distance modulus $m-M = 9.6$. This is consistent with our adopted reddening of $E(B-V) = 0.04$ together with the 100 K shift of the RYI grid. Demarque et al. estimate the error in the age to be +1.0 and −0.5 Gyr (Demarque et al. 1992). Our full sample of stars is shown on the H-R diagram in Figure 9*a* with the 3, 4, and 5 Gyr and ZAMS RYI isochrones of solar metallicity. The reader may find it slightly disconcerting that several dwarfs are displaced above the ZAMS. In this regard, we note the following. When plotted together with the entire cluster sample using the most recent and comprehensive CCD photometry of M67

TABLE 7

REDERIVED TEMPERATURES AND Li ABUNDANCES IN M67

Sanders	V	$B-V$	$T_{\rm eff}$ (K)[a]	log ϵ(Li)	ID
746.....	14.41	0.74	5540	<1.34[b]	I-46
747.....	14.05	0.70	5675	<1.60[b]	I-48
758.....	13.44	0.64	5910	2.34[c]	I-29
958.....	14.46	0.67	5970	<2.01[c]	I-160
976.....	13.12	0.61	6025	<2.09[d]	F132
988.....	13.19	0.58	6130	<1.82[d]	F129
990.....	13.41	0.59	6095	2.64[b]	I-20
994.....	13.20	0.57	6170	2.37[b]	I-9
995.....	12.77	0.56	6205	2.00[d]	F127
998.....	13.09	0.57	6170	2.47[b]	I-11
1092.....	13.33	0.63	5955	2.44[c]	III-43
1256.....	13.74	0.66	5830	1.10[b]	II-13
1292.....	13.23	0.62	5990	1.89[c]	III-22
1314.....	13.67	0.65	5870	2.42[c]	III-42
2205.....	13.16	0.58	6130	<2.21[d]	F128

[a] Effective temperatures were derived using the SH calibration for stars with $B-V \leq 0.63$ and the Böhm-Vitense 1981 calibration for stars with $B-V > 0.63$.

[b] Computed from equivalent widths taken from Hobbs & Pilachowski 1986b.

[c] Computed from equivalent widths taken from Spite et al. 1987.

[d] Computed from equivalent widths taken from García-López et al. 1988.

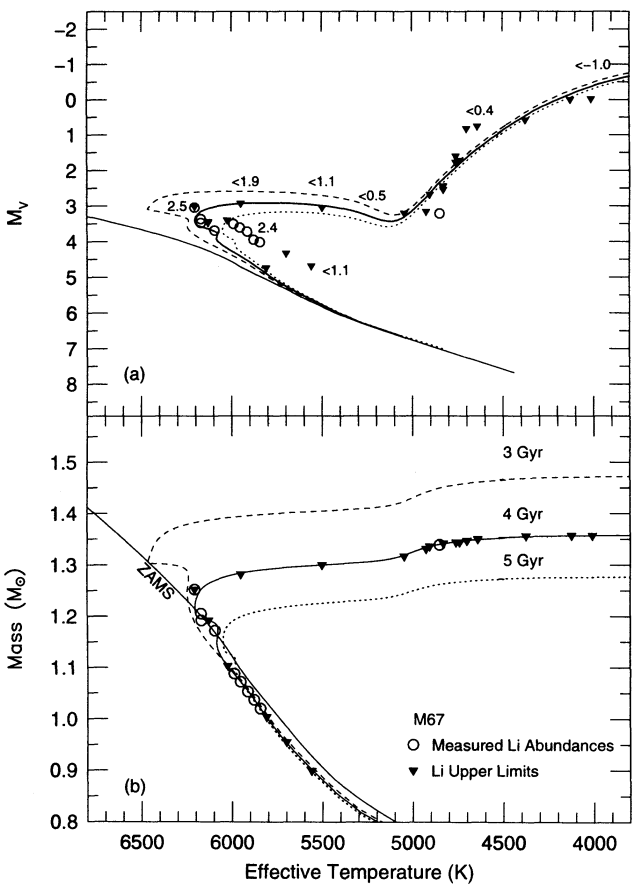

FIG. 9.—(*a*) M67 stars used in this study are shown on the H-R diagram with 3, 4, and 5 Gyr and ZAMS isochrones for [Fe/H] = 0.0 interpolated from the RYI grid. Typical Li abundances are indicated at several phases of evolution. (*b*) Masses of the same sample are shown as a function of $T_{\rm eff}$ with the same isochrones. Masses were derived from $T_{\rm eff}$'s using the 4 Gyr isochrone. Open circles are measured Li abundances, and filled triangles are Li upper limits.

(Montgomery, Marshall, & Janes 1993), we find that the stars observed for Li are among the brightest at a given color and lie along the upper envelope of, but are fully contained within, the main-sequence band which is ~1 mag wide. None of the stars in our sample is observed to be a double-lined binary. Two of the dwarfs below the main-sequence turn-off (I-29 and III-22) are single-lined binaries (D. W. Latham 1994, private communication), and these are displaced above the ZAMS in Figure 9. The remaining dwarfs may be single-lined binaries as well, but we have no information about this. Four single-lined binary turn-off and giant stars (F105, F111, F170, and I-20) lie on the 4 Gyr isochrone. We surmise that various observers have selectively picked the brightest stars for their abundance studies, thus accounting for their peculiar (but acceptable) position on the H-R diagram in our figure. We concluded earlier (§ 2) that due to the relative faintness of the companion, the lithium abundance estimate of the single-lined star should not be affected by its binary status. The masses of the individual stars were determined from their effective temperatures using the 4 Gyr isochrone. In Figure 9*b* mass is plotted as a function of temperature for the same set of isochrones. Since evolution is rapid past the cluster turn-off, there is only a small increase in stellar mass from the turn-off stars to the subgiants and giants. ZAMS temperatures were determined using the derived masses and the ZAMS solar-metallicity isochrone. These values are listed in Table 8.

The errors in the subgiant and giant masses resulting from the uncertainty in the age estimate of the cluster are the largest for M67. For a star at 5900 K just past the cluster turn-off, the mass estimate from the 4 Gyr isochrone is 1.29 $M_\odot$. The error in the age estimate of the cluster of +1.0 and −0.5 Gyr results in an uncertainty in the mass of −0.08 and +0.05 $M_\odot$. The ZAMS temperature of such a star is 6413^{-220}_{+165} K. This estimate of the errors in mass and ZAMS temperature applies uniformly to all of the subgiants and giants in M67.

TABLE 8

M67: MASSES AND ZAMS TEMPERATURES

Sanders	Mass ($M_\odot$)	ZAMS $T_{\rm eff}$ (K)
746	0.899	5482
747	0.955	5642
758	1.053	5862
794	1.331	6525
958	1.004	5758
976	1.103	5964
978	1.357	6606
986	1.252	6302
988	1.192	6155
989	1.344	6565
990	1.172	6110
994	1.192	6155
995	1.252	6302
998	1.205	6185
1001	1.336	6540
1010	1.350	6584
1016	1.356	6603
1034	1.282	6349
1092	1.072	5901
1231	1.317	6483
1239	1.300	6450
1250	1.357	6606
1254	1.344	6565
1256	1.020	5793
1279	1.347	6574
1288	1.344	6565
1292	1.088	5934
1293	1.342	6559
1305	1.342	6559
1314	1.037	5829
1463	1.339	6549
2205	1.192	6155

4. RESULTS

4.1. Li *Dip in* M67

We begin with an examination of Li depletion in M67. From a comparison of the meteoritic Li abundance (Anders & Grevesse 1989) with the maximum value seen in our reanalysis of the Hyades data, and in the Pleiades data of Soderblom et al. (1993a), it appears that there has been no significant increase in Li over the last 5 Gyr. The stars in M67 (which are of roughly solar age) can hence be assumed to have begun their main-sequence lives with a Li abundance of log ϵ(Li) ~ 3.0–3.3. In Figure 9, typical Li measurements or upper limits are marked for various stages of evolution. The dwarf data indicate that the Li abundance in stars just below the main-sequence turn-off is around log ϵ(Li) = 2.5, a depletion of ~0.5–0.8 dex from their initial abundance, which probably took place after the stars arrived on the ZAMS. The warmest subgiant in our sample is F111 with log ϵ(Li) < 1.90. By 5500 K, an upper limit of log ϵ(Li) < 1.1 is placed on F226. With the exception of III-57, which will be discussed separately, stars at the base of the red giant branch have log ϵ(Li) < 0.5. Ascending the red giant branch, giants show progressively smaller Li abundances consistent with their decreasing temperature and a roughly constant equivalent width limit.

Once a star evolves off the main sequence its convective envelope increases in depth and the mixing-in of Li-depleted material from the interior will dilute the surface Li abundance. However, this process is expected to be gradual, and since the convective envelope has to be deeper than the surface Li preservation zone before dilution can be observed, a decrease in Li is not expected to be observed until the star is at the base of the red giant branch. Dilution of about a factor of 50 is expected when the convective envelope has achieved its maximum depth (Iben 1967). In the standard stellar model, Li burning is not expected as the star ascends the red giant branch since the temperature at the bottom of the convective zone is not predicted to ever be hot enough. The observed decrease in Li in NGC 7789 giants as a function of evolution up the giant branch has been suggested as being due to Li burning (Pilachowski 1986), but this phenomenon has not been documented in other clusters and may conceivably be due to Li abundance differences established during the main sequence; the progenitors of the NGC 7789 giants are A stars, and in both the Hyades and the field, these show a large spread in Li (Burkhart & Coupry 1989, 1991). Thus, assuming concordance with theoretical predictions, the subgiants in M67 should retain their turn-off Li abundance of log ϵ(Li) ≈ 2.5, and the giants should show diluted Li abundances of about log ϵ(Li) = 0.8. The severe Li depletion exhibited by the subgiants immediately past the main-sequence turn-off, together with the factor of 1000 depletion in the giants is consistent with the hypothesis that these stars have undergone extensive depletion on the main sequence and have evolved from the Li dip region. The absence of any detectable Li in the M67 giants and the possible origin of these stars from the Li dip was first pointed out by Pilachowski et al. (1988). Since their data were

of lower S/N, they added together the spectra of several giants at roughly the same temperature. Our higher quality spectra confirm their result unambiguously, and the lack of Li in the subgiants as well is stronger evidence that the stars have indeed evolved from the dip.

We draw particular attention to the fact that Li is not detected in the subgiants just past the turn-off. Since the depth of the surface convective zone is expected to begin increasing once the star leaves the main sequence, any lithium which has diffused below the surface convective zone during the main-sequence life of the star will be immediately dredged up in these stars. The Li abundances in the turn-off subgiants would then be close to log ϵ(Li) = 2.5. The upper limits of log ϵ(Li) < 1.9 in F111 and especially of log ϵ(Li) < 1.1 in F226 are hence extremely significant and indicate the absence of subsurface lithium. Our observations indicate that Li in the dip stars has been destroyed at least to the level of our upper limits. The importance of these observations in the context of theoretical models which purport to explain the Li dip will be discussed in § 5.

The detection of Li in III-57 requires further comment. The value of the Li abundance itself is not abnormal; III-57 has a Li abundance of log ϵ(Li) = 0.85, consistent with the Hyades stars in the middle of the Li dip which have upper limits of log ϵ(Li) < 1.4. The Li detection in III-57 is enigmatic only in the context of nondetections in subgiants less evolved and giants more evolved than it. Do all of the dip stars retain Li at this abundance? It could be argued that such an abundance would result in too small an equivalent width to be detected in our hotter subgiants F111 and F226. Giants more evolved than III-57 are expected to have undergone dilution through dredge-up and thus have lower abundances. The maximum Li abundance expected as a result of dilution in a giant which left the main sequence with an abundance of log ϵ(Li) = 0.85 is log ϵ(Li) = −0.90. Within the errors, all of the upper limits in our giants can be accomodated as a consequence of dilution. The greatest challenge to the normality of III-57 comes from the three stars which bracket III-57 in temperature and evolutionary phase: IV-77, I-17, and II-22. All of these stars have Li upper limits ~0.35 dex below the detection in III-57. Their spectra were taken during our most recent Kitt Peak run expressly for the purpose of comparison with III-57 and the S/N and resolution are among the highest in our sample. The absence of detectable Li in IV-77, which is at an identical stage of evolution as III-57, suggests that the abundance seen in III-57 is not, for example, the result of dredge-up unique to this phase of evolution. III-57 does not appear to be unusual in any other way; for example, a high level of chromospheric activity, which has previously been linked in field giants to larger than average Li abundances (Randich, Gratton, & Pallavicini 1993; Fekel & Balachandran 1993), is not seen in III-57 (L. Pasquini 1994, private communication). Thus the detection of Li in III-57 together with the absence of Li in IV-77, I-17 and II-22 argues strongly for the existence of a spread in the Li abundances in stars in the Li dip.

4.2. *Comparison of the Hyades and Praesepe Clusters*

Li abundances are plotted as a function of effective temperature for the stars in the Hyades and Praesepe clusters in Figure 10*a*. Our initial examination of Praesepe was motivated by the differences between the Hyades and Praesepe G dwarfs ($T_{\rm eff}$ < 5800 K) observed by Soderblom et al. (1993a, Fig. 4). It was hence most striking to us that these differences vanish when the two clusters are placed on the same temperature calibration scale and subjected to the same abundance analysis. Below 5800 K, the Praesepe stars follow the same sharp decline in Li seen in the Hyades. With the exception of KW 540, which stands out above the mean trend, and KW 392, which is well below the mean trend, stars in Praesepe *do not* show larger abundances than the Hyades as seen by Soderblom et al.

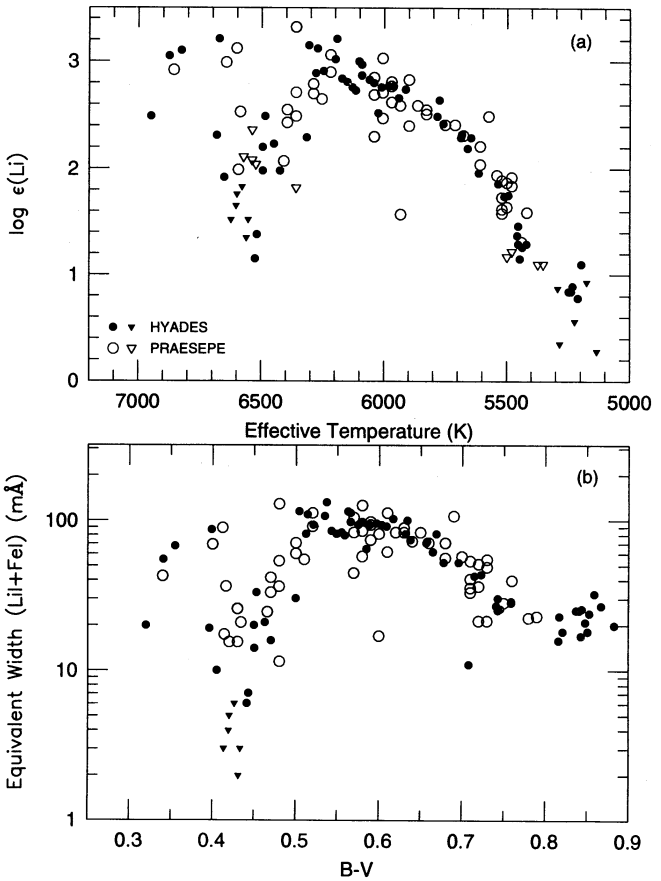

FIG. 10.—(*a*) Equivalent widths (Li I + Fe I blend) as a function of $B-V$ and (*b*) Li abundances as a function of $T_{\rm eff}$ in the Hyades (*filled symbols*) and Praesepe (*open symbols*) clusters. Triangles represent upper limits to the Li abundance in both clusters.

Soderblom et al. suggested that the observational plane of equivalent width versus color is more suitable for cluster comparisons because the errors in these quantities are better understood, and their Figure 1 shows apparent differences between the Hyades and Praesepe clusters. We note, however, that the quantities they plot are not purely observational; the Li I equivalent width has been deblended from the observed feature which contains Fe I + CN as well. The different deblending procedures used in the Soderblom et al. study for Praesepe and in the Thorburn et al. (1993) study for the Hyades (discussed in §§ 3.3 and 3.4) result in systematically smaller Li I equivalent width measurements in the cooler Hyades stars of the same color. Since the strength of the contaminating Fe I + CN blend is small in the F stars, differences between the two clusters were only seen in the G dwarfs. We plot the (measured) blended Li I equivalent widths (Li I + Fe I + CN) from the two studies as a function of $B-V$ for both clusters (Fig. 10*b*). No difference between the two

clusters is seen in this observational plane, further substantiating our claim that the clusters appear identical.

The differences between the Hyades and Praesepe seen by Soderblom et al. (1993a) are thus due to a combination of the systematic differences in the Li I deblending procedures in the two clusters and the use of $V-I$ colors to derive temperatures in Praesepe. The $V-I$ colors of Mendoza (1967) show a larger scatter suggestive of larger photometric errors, and this color is more susceptible to contamination by an unseen binary companion.

The similarity between the Praesepe and Hyades clusters continues to be very strong in the hotter stars. Both clusters show a spread in Li between 5800 and 6300 K. The spread is larger in Praesepe, but this may be due to the superior quality Hyades data which were taken by Thorburn et al. (1993) expressly for the purpose of minimizing errors. If cluster-to-cluster variations in this temperature range are to be investigated, a closer inspection of Praesepe may be required as well.

The Li dips in both clusters appear identical. At the hot end, abundances drop sharply at $\sim$6650 K in both clusters, and the rise from the dip at cooler temperatures is more gradual. In fact, Praesepe stars neatly fill the temperature gap in the Hyades dip between 6350 and 6400 K. There is a hint that the hot edge of Praesepe may be slightly cooler than the Hyades, but this cannot be firmly established with the current small sample and the errors in temperature determination. The Praesepe dip appears shallower than the Hyades only because the lower S/N data in the fainter Praesepe stars result in larger upper limits at the bottom of the dip.

Our finding that the Li versus $T_{\rm eff}$ distributions in the Hyades and Praesepe clusters, which are of the same age but different metallicities, are identical casts serious doubt on Swenson et al.'s (1994) explanation that the Li versus $T_{\rm eff}$ distribution in the Hyades can be produced by pre–main-sequence depletion alone. Their explanation rests on producing greater pre–main-sequence depletion in the higher metallicity Hyades cluster via an increase in the interior opacities and would imply that G dwarfs in Praesepe should have a larger Li abundance than Hyads at the same temperature, unless their oxygen abundances are extraordinarily high. Analysis of a larger sample of Praesepe stars is crucial to confirm Friel & Boesgaard's (1992) finding that Praesepe does indeed have a smaller metallicity than the Hyades.

4.3. *Comparison of the Hyades, Praesepe,* NGC 752, *and* M67 *Clusters*

Li abundances in the Praesepe, NGC 752, and M67 clusters are plotted as a function of mass (Fig. 11) and as a function of ZAMS temperature (Fig. 12). The Hyades abundances are plotted in most of these figures to facilitate easy comparison. Our basic goal is to decipher changes in the shape of the Li dip with age and with metallicity. The systematic errors in the masses and ZAMS temperatures of NGC 752 and M67 stars, which arise from the estimated uncertainties in the cluster age determinations discussed in §§ 3.5 and 3.6, are marked on the appropriate figures. These errors apply to the four highest mass NGC 752 stars and to all the subgiants and giants in M67. For the remaining stars, the relative errors in masses and ZAMS temperatures with respect to older or younger clusters are negligible.

The center of the Li dip is located at $\sim 1.4\ M_{\odot}$ in the Hyades (Fig. 11*a*). Relative to the Hyades, the M67 dip extends to lower masses. Has the Li dip widened with age as several theoretical explanations for the dip have predicted? Within the possible systematic error of $+0.05$ and $-0.08\ M_{\odot}$ in the masses of the subgiants and giants, the M67 dip may well be coincident with the Hyades, and the apparent shift may not be real. (A comparison with Praesepe will later show that the errors in the masses of M67 can be reduced substantially.) Further, since the blue edge of the Li dip cannot be clearly defined in M67, its center is impossible to place, and conclusions about whether the dip has merely shifted in mass or become wider cannot be drawn. A possible shift in the mass of the Li dip can be better addressed by comparing the Hyades and NGC 752 clusters (Fig. 11*b*). With the blue edge of the NGC 752 dip "well" defined, its center can be reliably placed at $\sim 1.22\ M_{\odot}$. Note that the uncertainty in the masses of the four turn-off stars in NGC 752 does not affect the mass of the Li dip center. Since the 2 Gyr NGC 752 cluster is younger than M67, the shift in the mass of the Li dip between the Hyades, M67, and NGC 752 is not due to age, but must be related to metallicity alone; NGC 752, the lowest metallicity cluster, has the dip with the smallest mass. It should be noted that despite the larger errors in M67, the mass at the center of the NGC 752 Li dip is clearly outside the range allowed for M67 (Figs. 11*a* and 11*b*).

The comparison can be extended to Praesepe and the Hyades. Although these clusters are of roughly the same age, the Praesepe dip, centered at $\sim 1.32\ M_{\odot}$, is clearly at a lower mass than the Hyades (Fig. 11*c*), lending further support that the difference is related to metallicity alone. It is of interest to note that at a given mass, the lower metallicity Praesepe stars have undergone less depletion than the higher metallicity Hyades stars at the same age (Fig. 11*c*). The shift in the mass of the Li dip due to metallicity was first remarked upon in our study of field F dwarfs (Balachandran 1990a) based on a rough binning of the stars into metallicity groups. The cluster data show the same characteristic in a much clearer fashion and are qualitatively consistent with the field star findings.

Assuming that the mass at the center of the Li dip is dependent only upon the metallicity of the star, Praesepe can be used to set the errors in the position of the M67 dip. Allowing for the slightly lower metallicity of M67 relative to Praesepe, the M67 dip should be centered at $\sim 1.30\ M_{\odot}$ (Fig. 11*d*). The M67 giants with the lowest Li abundances are at $1.35\ M_{\odot}$. If these giants define the center of the M67 Li dip, then the cluster age must be underestimated by 0.5 Gyr. An overestimate in the cluster age seems unlikely since it would imply that the highly depleted giants have evolved from temperatures hotter than the dip. Alternatively, the 4 Gyr estimated age of the cluster may be accurate, in which case the Li dip is centered at the base of the red giant branch, and the giants would then have evolved from the blue side of dip. The possible error in the masses of the M67 subgiants and giants is reduced by this comparison to $+0.00$ and $-0.04\ M_{\odot}$, and the error in ZAMS temperatures decreases to $+0$ and -110 K.

Balachandran's (1990a) field star study indicated that the Li dip is at roughly the same ZAMS temperature irrespective of the metallicity of the star. Again, the cluster data may provide a more definitive conclusion. In Figure 12*b* the most striking feature, though based on a small sample in NGC 752, is the near-perfect alignment of the blue edge of the Hyades and NGC 752 dips. Note that the four NGC 752 stars, which have larger uncertainties in their masses and hence ZAMS temperatures due to the uncertainty in the cluster age, do not play a role in defining the blue edge of the dip. Let us define the blue

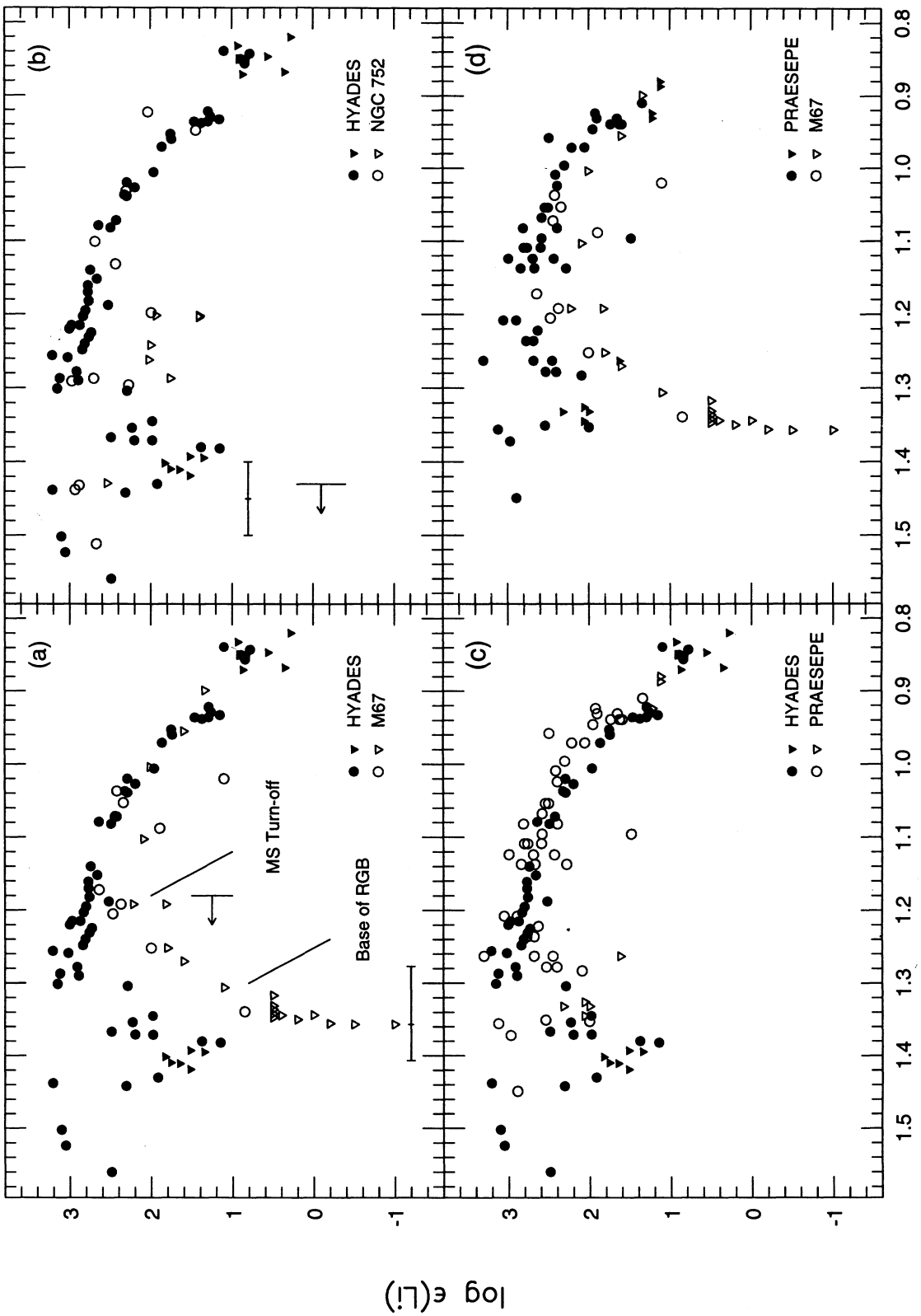

FIG. 11.—Li abundances as a function of mass for: (*a*) Hyades (*filled symbols*) and M67 (*open symbols*). The error bar indicates the uncertainty in the mass determination resulting from the uncertainty in the age estimate of M67 and applies only to those stars equal to or more massive than the limit indicated by the arrow. (*b*) Hyades (*filled symbols*) and NGC 752 (*open symbols*). Error bar and arrow as above, but in this case for NGC 752. (*c*) Hyades (*filled symbols*) and Praesepe (*open symbols*). (*d*) Praesepe (*filled symbols*) and M67 (*open symbols*). In each case, circles represent measured Li abundances, and triangles upper limits.

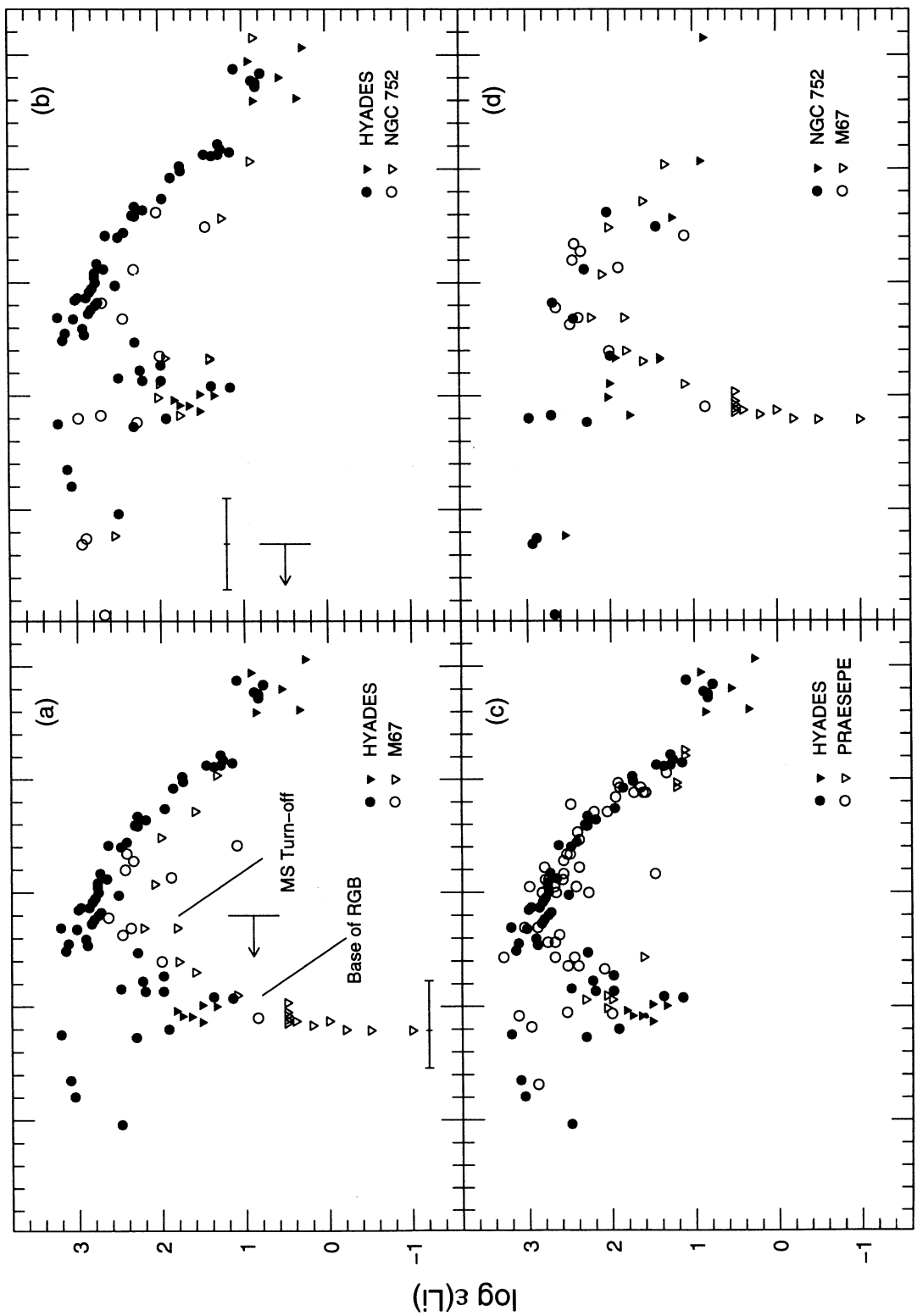

FIG. 12.—Li abundances as a function of ZAMS $T_{\rm eff}$ for: (*a*) Hyades (*filled symbols*) and M67 (*open symbols*). The error bar indicates the uncertainty in the ZAMS $T_{\rm eff}$ resulting from the uncertainty in the age estimate of M67 and applies only to those stars equal to or hotter than the limit indicated by the arrow. (*b*) Hyades (*filled symbols*) and NGC 752 (*open symbols*). Error bar and arrow as above, but in this case for NGC 752. (*c*) Hyades (*filled symbols*) and Praesepe (*open symbols*). (*d*) NGC (*filled symbols*) and M67 (*open symbols*). In each case, circles represent measured Li abundances, and triangles upper limits.

edge of the Li dip as the temperature range over which Li drops by a factor of 20. This abundance drop is bracketed by three stars in each of the Hyades and NGC 752 clusters. The effective temperatures of the blue edges of the Hyades and NGC 752 Li dips are 6620 ± 18 K and 6601 ± 15 K, respectively, a very good match indeed. Four stars define the blue edge of the Praesepe dip, which is at 6550 ± 29 K. Given the errors in temperature determinations and the small numbers of stars involved, the blue edges of the Hyades and Praesepe Li dips are in reasonable agreement. Thus, not only are the Hyades and Praesepe, which are of roughly the same age, well aligned at the blue edge of the dip, but there is little change in the width or slope of the dip at the blue edge between 750 Myr and 2 Gyr. Further, no shift in the ZAMS temperature of the Li dip is discerned as a result of the metallicity differences between the clusters. A comparison of the Hyades and Praesepe clusters (Fig. 12*c*) shows a good match on the red side of the Li dip as well. The red edges of the Hyades and NGC 752 clusters are not as well matched. Based on the few NGC 752 stars between 6100 and 6350 K, the red side of the Hyades dip is steeper than NGC 752. While this may indeed be the result of the Li dip widening with age, it should be noted that G dwarfs at temperatures cooler than 6000 K have systematically lower Li abundances in NGC 752 than in the Hyades (Fig. 12*b*), probably due to main-sequence depletion which has occurred after the age of the Hyades. Thus the appearance of the wider Li dip may merely be the result of a decrease in the Li plateau level of stars around 6200 K by some depletion mechanism unrelated to the dip. It could be argued that stars in NGC 752 had a lower initial Li abundance at the time of formation, thus requiring no main-sequence depletion to account for their present abundances being lower than the Hyades. On the basis of well-determined meteoritic and Hyades early-F star abundances which suggest the absence of Li enhancement over the last 5 Gyr, we deem this to be less likely. However, Li abundance measurements in NGC 752 turn-off stars would be invaluable to constrain the initial abundance in the cluster and hence from the basis for understanding main-sequence Li depletion. In this regard it is interesting to note that, similar to NGC 752, the dip is wider in M67 than in the Hyades (Fig. 12*a*).

The red edges of the NGC 752 and M67 dips are closely matched in ZAMS temperature (Fig. 12*d*). The error in the ZAMS temperatures of the M67 dip stars due to any uncertainty in the cluster turn-off age has been earlier constrained by comparison with Praesepe to be at most −110 K. A shift of the M67 dip to a higher ZAMS temperature is thus unlikely. Recognizing this constraint, we suggest that there has been very little change in the Li abundances of these stars (ZAMS $T_{\rm eff} \sim 6000$–6300 K) beyond the age of 2 Gyr. With somewhat lesser certainty, because of the larger scatter, we suggest that there has also been little change in the Li abundances of the cooler G dwarfs ($T_{\rm eff} \sim 6000$–5500 K) between 2 and 4 Gyr. Additional G dwarf spectra in both clusters would be invaluable. Thus the temperature of the red edge of the Li dip appears to show no shift with metallicity either; the observed change between the Hyades and NGC 752 is probably a result of age alone.

In the light of the Li detection in III-57, which led to our conclusion that a spread in Li exists in the M67 Li dip, it behooves us to look for a similar effect in other clusters. Since the dip stars in the other clusters are on the main sequence, they are hotter, and high-S/N spectra are required to look for a scatter among their low Li abundances. In NGC 752, for example, only upper limits have been placed on stars at the bottom of the Li dip. The best data are for the Hyades. Four stars near the bottom of the Hyades dip have Li measurements of $\log \epsilon(\mathrm{Li}) = 1.45$ and 1.55 and upper limits of $\log \epsilon(\mathrm{Li}) = 1.40$ and 1.50. All four stars are within a temperature range of ~50 K. Recall that the upper limits are conservative estimates which assume no contribution by the Fe I λ6707.4 blend. Thus, while the evidence for a spread in Li is not as strong in the Hyades as in M67, it is conceivable that a similar spread may exist. It is clear, however, that the mechanism which is responsible for the Li dip dominates the depletion of Li in all of the dip stars. *No star within the temperature interval that defines the Li dip escapes Li depletion, and any regulation of the extent of depletion by other stellar parameters is only secondary.* Note that the measured abundances near the bottom of the Hyades dip are larger than in III-57, suggesting that the Li depletion continues between the ages of the Hyades and M67.

5. COMPARISON WITH THEORETICAL MODELS

Armed with our own observations of M67 and the complete reanalysis of the published cluster data, we proceed to investigate agreements and conflicts with theoretical models. The principal observational facts assembled from our analysis are as follows:

1. Li in stars in the dip has been effectively destroyed.
2. The mass at the center of the Li dip increases with increasing metallicity.
3. The ZAMS temperature at the center of the Li dip is independent of metallicity.
4. There is some evidence for a spread in Li in stars in the dip.
5. The morphology of the Li dip is characterized by a sharp drop at the blue edge and a more gradual rise at the red edge.
6. There is no change in the ZAMS temperature or shape of the blue edge with age. The red edge becomes less steep with age; this may either be caused by an evolution in the Li dip, or by a decrease in Li in stars cooler than the red edge and thus unrelated to the Li dip phenomenon.
7. At the same age, the shape of the Li dip in the Li versus $T_{\rm eff}$ plane is independent of the metallicity of the cluster.

Six theoretical models contest the right to explain the Li dip. Of these models, mixing by internal gravity waves suggested by García-López & Spruit (1990) is not considered in detail here. We note that the authors found it necessary to increase the intensity of the waves by a factor of 15 to match the depletion observed in the dip. The mixing capabilities of these waves remain to be investigated more thoroughly before comparisons with observations can be performed.

It is useful to keep in mind the structure of the Li dip stars through the course of the discussions which follow. In the standard stellar model, lithium survives in the outer few 2%–3% by mass of F and G dwarfs (Iben 1967) through the entire main-sequence life of the stars. While this Li preservation zone has a fairly constant fraction across the F and G dwarf spectral range, the mass of the surface convective zone changes drastically, and the change is especially large in the F stars; the convective zone increases from 10^{-8} to $10^{-3}\ M_\odot$ from 7200 to 6400 K (Michaud 1986). Thus, for a typical Li dip star at 6600 K, the surface convective zone is at most a few percent by mass of the Li preservation zone.

5.1. *Microscopic Diffusion*

The earliest, and the most elegant explanation for the Li dip was the microscopic diffusion model of Michaud (1986) which predicted that Li would settle gravitationally out of the convective zone in stars with $T_{\rm eff} < 6900$ K. At hotter temperatures, upward radiative acceleration was predicted to dominate over gravitation, leading to surface Li enrichment. To explain the lack of Li enhancement observed in hotter stars, Michaud (1986) invoked the ad hoc, but modest and not unreasonable, mass-loss rate of $\dot{M} = 10^{-14}\,M_\odot\ {\rm yr}^{-1}$. The lack of Li depeletion in stars cooler than $\sim$6400 K, i.e., the rise on the cool side of the Li dip, was argued as being due to the longer timescale required to drain the deeper convective envelopes of these stars. Thus the dip was expected to widen with age. Since the initial study which involved only a static stellar model, Proffitt & Michaud (1991) and Richer, Michaud, & Proffitt (1992) have constructed fully coupled stellar evolution and diffusion models. The most sophisticated treatment was presented in the recent study of Richer & Michaud (1993) which utilized the new OPAL opacities (Rogers & Inglesias 1992) and simultaneously solved for stellar evolution and diffusion in a nonrotating stellar model, treating the stellar envelope as inhomogeneous with He and trace element diffusion. While mass loss was not included in their study, and thus their predictions for the hot stars were not expected to match observations, the abundances of the dip stars were expected to be predicted accurately.

Our observations in M67 subgiants and giants present the principal and most severe contradiction to the microscopic diffusion hypothesis. According to the models, gravitationally settled Li is supported in a region just below the convective zone and is dredged up to the surface as soon as the star evolves off the main sequence (see Fig. 7 in Richer & Michaud 1993). Thus while the dip star appears Li-depeleted on the main sequence, it should be indistinguishable from lower or higher mass stars once it is at the cluster turn-off. In M67 no dredge-up of Li is seen at the main-sequence turn-off or later on the subgiant branch; our observations indicate that Li in the dip stars has been destroyed. It is conceivable that once Li settles out of the surface convection zone, some other process may be responsible for transporting it to stellar interior where it is destroyed. Assuming that such a process does not inhibit gravitational settling (and this will have to be examined once the process is identified), we proceed with more detailed comparisons of the observations with the Richer & Michaud (1993) predictions.

The temperature at the hot edge of the Hyades dip, as defined by the SH calibration, is in good agreement within $\sim$50 K with the Richer & Michaud (1993) prediction for 800 Myr. The cool edge of the dip is, however, cooler than predicted, and thus overall the predicted dip is narrower than observed. Also, the predicted shape of the cool edge of the dip does not match observations, which shown a more gradual rise from the bottom of the dip. Both the narrow width of the dip and the square shape of the cool edge, which are different from the initial prediction of Michaud (1986) based on the static stellar model, are the result of the more sophisticated modeling by Richer & Michaud (1993) which includes helium settling.

Richer & Michaud (1993) find that, at a given age, the temperature of the Li dip varies with metallicity when the OPAL opacities are used, but not when the older Los Alamos (Huebner et al. 1977) and Kurucz (1990) opacities are used. With the OPAL opacities, the shift in temperature was predicted to be between 40 and 80 K for a metallicity difference of 0.18 dex. Thus the difference should be $\sim$60–130 K between the Hyades and NGC 752, with the Hyades Li dip being cooler. While a difference of 60 K cannot be ruled out with the existing data, the remarkable coincidence in ZAMS temperatures of the bulge edge of the dip in the Hyades and NGC 752 makes the larger difference unlikely (Fig. 12*b*). Since our ZAMS temperatures were obtained from masses derived via the RYI which utilized older opacities, some doubt may be entertained about their ability to reflect true ZAMS temperatures with the desired accuracy. A similar comparison of the Hyades and Praesepe clusters, which are of roughly the same age, can be carried out by simply using the present temperatures of the stars, thus avoiding uncertainties introduced by the choice of isochrones. A marginal shift in the hot edge of the Li dip is seen between the two clusters (Fig. 10*a*) but in the opposite sense to the Richer & Michaud prediction; the lower metallicity Praesepe cluster is cooler than the higher metallicity Hyades. Thus the predicted displacement of the dip with metallicity is not reflected in the data, although, since the shift is small, it cannot be ruled out completely.

There are other observations which must be addressed by the diffusion hypothesis. García-López et al. (1994) point out that there is no difference in the oxygen abundances of Hyades F stars inside and outside the Li dip. While the enhancement or depletion of elements other than Be have not been predicted for the dip stars, Michaud (1986) suggests that these may be inevitable. Calculations for oxygen are awaited with interest. Burkhart & Coupry (1989, 1991) have found a spread of $\sim$1.0 dex in Li in Hyades A stars. The magnitude of the depletion did not depend on whether the star was an A or an Am star. According to Richer & Michaud's (1993) calculations the surface Li abundance of a star hotter than the Li dip is a complex function of its mass and evolutionary status. While a surface Li enhancement is predicted for stars between 1.44 and 1.5 $M_\odot$, more massive stars (1.5–1.8 $M_\odot$) are predicted go through rapid high and low surface Li oscillations during their main-sequence lifetime as a result of their extremely thin convective zones and rapid evolutionary timescales. We surmise that, even in the absence of mass loss or any other mechanism that may inhibit gravitational settling, this makes it difficult to predict the Li abundance of a given A star; perhaps some light may be shed in a detailed comparison with other abundance anomalies in the star.

5.2. *Models Involving Rotation*

Several models which explain the Li dip do so by recognizing that the dip occurs in the temperature domain which roughly defines the boundary between stars with and without surface convective envelopes, and by utilizing the unique properties of stars which span this region. Most important among these is that all stars cooler than the dip undergo rapid rotational spin-down, while the presence of rapid rotators among the relatively old field stars suggests that stars hotter than the dip retain a large fraction of their initial rotational velocities through their main-sequence lives. The average rotational velocities of stars thus show a sharp decline across this region.

5.2.1. *Meridional Circulation*

Rapid rotation is known to produce meridional circulation currents (Eddington 1925; Sweet 1950). Its effectiveness in producing mixing in F stars was examined by Charbonneau &

Michaud (1988) by extending the A star meridional circulation models of Tassoul & Tassoul (1982) which assume solid-body rotation. Assuming that the presence of the surface convection zone has no effect on the circulation pattern below it, they predicted that rapid rotation would inhibit microscopic diffusion. The critical rotational velocity required varied strongly with the temperature of the star. Thus, in their model, meridional circulation could replace mass loss as the mechanism preventing Li enhancement in rapid rotators ($v > 50$ km s^{-1}) hotter than the dip. In the dip stars, depletion could either be the result of grativational settling (for $v < 15$ km s^{-1}) or meridional circulation (for $v > 20$ km s^{-1}). At temperatures lower than 6400 K, gravitational settling was found to be inhibited in all except the slowest rotators ($v < 5$ km s^{-1}) providing a stronger constraint than merely timescale to account for the rise in Li on the cool side of the dip. While not explicitly stated in Charbonneau & Michaud (1988), we surmise that in this picture the Li dip would not widen with age.

Since meridional-circulation–related mixing has implications on Li abundances outside the temperature of the Li dip, it is important to recognize several observational disagreements with the predictions of this hypothesis. Some of these are discussed in Charbonneau & Michaud (1988). The most severe contradiction, unrelated to the Li dip, is seen in the early F dwarfs in the field (Balachandran 1991a). Stars with $v < 50$ km s^{-1} are predicted to show Li enhancement by factors of 2–8 due to the domination of radiative acceleration, and more rapid rotators are predicted to show Li depletion through meridional circulation; such a correlation is not observed. The meridional circulation hypothesis would suggest that the stars on the hot side of the Hyades dip with velocities less than 50 km s^{-1} should be overabundant in Li. While such an overabundance may have been deduced from the abundances derived by BB, the SH temperature calibration equalizes the Li abundances in Hyades stars hotter and cooler than the dip. Since the stars in the Hyades dip show a spread in rotational velocities, Li depletion via meridional circulation alone would be expected to produce a scatter in Li abundances which Charbonneau & Michaud (1988) point out is not observed. The lack of a scatter in the well-defined Hyades dip is not in itself an argument against the hypothesis since gravitational settling can be invoked to explain Li depletion in stars with low rotational velocities; the combination of gravitational settling and meridional circulation could produce the observed sharp dip in the Hyades. The result of such a process would lead to an observable spread in Li when these stars evolve to become red giants. The giants whose progenitors were slow rotators will dredge up their gravitationally settled Li, while those whose progenitors were rapid rotators and underwent destruction via meridional circulation will not.

Charbonneau, Michaud, & Proffitt (1989) suggested that meridionally circulated material in the stellar interior may not penetrate the surface convective zone of the main-sequence star if a shielding boundary layer develops between the radiative interior and the convective zone. In such a case, the star will appear normal during its main-sequence life, but the mixing it has undergone in its interior will be revealed during the subgiant and giant phases. Recall that since the surface convective envelope of the mid-F star is only a few percent of the Li preservation zone within the star, mixing in the interior and depletion of this preservation zone can lead to substantially lower Li abundances in giants compared to the canonical maximum dilution of a factor of 50–75 from the observed main-sequence abundance. The latter, of course, is derived from the assumption that the entire Li preservation zone has the same abundance as the surface. While a shield between the interior and the surface convective zone cannot account for the main-sequence Li dip, Charbonneau & Michaud (1990) suggested that this hypothesis may explain the low Li abundances in M67 and NGC 752 giants. Our analysis has shown that the M67 giants have evolved from the temperature of the Li dip, and hence meridional circulation which does not penetrate the surface convective zone of the main-sequence star is not an acceptable explanation for these stars. However, interior mixing on the main sequence could provide a solution to the low Li abundances in NGC 752 giants (Pilachowski, Saha, & Hobbs 1988; Gilroy 1989) which are puzzling because their main-sequence progenitors are not expected to have undergone Li depletion according to the standard stellar models. Observations of giants in other clusters (Gilroy 1989) show that the low Li abundances seen in NGC 752 giants are not a rarity even in giants of greater than 2 $M_\odot$. Although Gilroy's (1989) sample in each cluster is small, there appears to be a scatter in Li abundances within each cluster which could, for instance, be explained by variable internal mixing. It should be noted that while detailed calculations were not performed, Charbonneau & Michaud (1989) suggested that a correlation between $^{12}C/^{13}C$ isotope ratios and Li abundances was likely if meridional circulation was the depleting mechanism. Such a correlation was not observed by Gilroy (1989). The progenitors of the NGC 752 giants were late-A stars on the main sequence which Burkhart & Coupry (1989, 1991) noted show a spread in Li in the Hyades. Conceivably these stars hold the clue to the low giant abundances.

We conclude that there appears to be an overall lack of agreement between observations and predictions of the meridional circulation hypothesis in F stars, at least as modeled by Charbonneau & Michaud (1988).

5.2.2. *Turbulent Diffusion*

The Tassoul & Tassoul (1982) formulation of meridional circulation adopted by Charbonneau & Michaud (1988) retained only the first-order Ω^2 term (where Ω is the angular velocity). Inclusion of the second-order Ω^2 term leads to the splitting of the meridional circulation pattern into an outer and an inner loop separated by a "quiet zone" which effectively decouples the two. Using this formulation, Vauclair (1988) and Charbonnel, Vauclair, & Zahn (1992) were able to explain the Li dip by predicting that the inner loop would lie within the surface convective zone for stars cooler than 6600 K, thus leading to large surface Li depletion. In hotter stars, the surface convection zone moves outward, the inner loop lies in the radiative zone, and the quiet zone is expected to shield the surface from Li-depleted material.

The principal theoretical objection to this model is that the quite zone would not prove to be an effective shield (Charbonneau & Michaud 1990). Microscopic diffusion was predicted to take place across the quiet zone, leading to large Li depletion on the surfaces of hot stars, contrary to observations. To counter this problem, Charbonnel & Vauclair (1992) decreased the efficiency of turbulent diffusion by a factor of 1000 in the outer zone relative to the inner zone. Thus Li depletion continued with the same efficiency in the interior, but transport to the outer zone was reduced to match observations. However, no theoretical basis was cited for the change.

Since the position of the quiet zone varies with rotational velocity, being deeper for faster rotators at a given mass, the model can produce the low Li abundances seen in giants and explain their scatter as being due to mixing to varying depths within the stellar interior. Moreover, since extensive depletion of Li is predicted to have occurred in regions just below the thin surface convective zone, a modest increase in its depth would be sufficient to dredge up Li-depleted material and account for the low Li abundances in M67 subgiants. Since the model has been adjusted to fit the Li dip, its merit may have to be determined by comparison with other observations, for example, consistency with observed $^{12}C/^{13}C$ ratios in giants. Charbonnel (1994) has shown that the standard stellar models are able to predict the observed $^{12}C/^{13}C$ ratios in M67 giants up to the first dredge-up phase. The CNO profile built up during the main-sequence phase is hence adequately represented by the standard model, and main-sequence mixing must be constrained to a depth less than that affected by CNO processing. Theoretical predictions for the depth of mixing in the Vauclair (1988) model are awaited.

The principal observational conflict arises from the comparison of theoretical predictions with the observed Hyades Li dip. According to the model, the position of the quiet zone and hence the extent of Li depletion is a strong function of the rotational velocity of the star. While Charbonnel et al. (1992) claimed good agreement between their predictions and the observed cool edge of the Hyades dip (see their Fig. 3*c*), the assumptions made in order to produce the fit should be recalled. All stars were assumed to arrive on the main sequence with a rotational velocity of 100 km s^{-1}. This is unreasonable because young cluster data show that a large fraction of stars arrive as slow rotators on the main sequence and the initial velocity of 100 km s^{-1} or larger is seen in at most one-third of the stars (Stauffer 1991). In order to fit the observed Hyades Li distribution, the final rotational velocities are constrained to lie within a narrow band which declines sharply across the region of the Li dip as indicated by curves 2 and 3 in their Figure 3*b*. The observed rotational velocities (admittedly v sin i) show a larger spread of 10–60 km s^{-1}, which would result in a much larger spread in Li than is observed, with a large fraction of the Hyades dip stars not having undergone any Li depletion at all.

5.2.3. *Rotational Braking*

Extending the initial calculations of Endal & Sofia (1981), Pinsonneault et al. (1989) suggested that Li depletion on the main sequence was the result of turbulent mixing caused by rotational spin-down. According to their models (Pinsonneault et al. 1990), the extent of mixing depends upon the magnitude of the spin-down; thus main-sequence stars of the same mass and the same initial Li abundance but with a range in initial angular momentum will exhibit a spread in Li after they have all spun down to the same final velocity. In their models, the extent of mixing also depends upon the mass of the star in a complicated fashion (see Figs. 12 and 13 in Pinsonneault et al. 1990): at a small initial angular momentum (J_0), higher mass ($\sim 1.2\ M_\odot$) stars undergo almost no Li depletion relative to solar-mass stars; at intermediate J_0, depletion is almost uniform with mass; and at high J_0, 1.2 $M_\odot$ stars undergo more extensive depletion than solar-mass stars.

Pinsonneault et al.'s (1990) explanation for the Li dip rests on an interpretation of the data that the observed rotational velocity distribution in T Tauri stars and solar-type stars in young clusters is skewed toward smaller values compared to higher mass stars. Two assumptions were made based on these observations: first, that the initial rotational velocity of the solar-type stars is represented by the observed distribution in young clusters, and second, that the difference in the rotational velocity distributions between the low- and high-mass stars occurs sharply at the cool edge of the Li dip. The dip is then explained by the increased Li depletion in the higher mass stars which, *on average*, have undergone a greater magnitude of spin-down.

The origin of the angular momentum distribution in young clusters is not well understood. For instance, the T Tauri distribution cannot be evolved to look like that in young clusters without some ad hoc assumptions about the rates of angular momentum loss on the pre–main-sequence (Bouvier 1991). Furthermore, the observed velocity distributions in young clusters may have been altered rapidly since their arrival on the main sequence, especially in the F and G stars with extremely thin outer convective envelopes. Even allowing for the validity of the assumption that the rotational velocity distributions in high- and low-mass stars are intrinsically different, there is no compelling observational evidence that the distribution changes sharply at 1.2 $M_\odot$, the cool edge of the Li dip (Soderblom et al. 1993d). The theoretical basis for Pinsonneault et al.'s (1990) assumption is derived from Kawaler's (1987) reexamination of the Kraft (1970) rotation curve for high-mass stars and its extrapolation to lower masses. That extrapolation, which resulted in the sharp change in initial angular momentum at 1.2 $M_\odot$, was based on theoretical stellar models which predict that the relationship between radius and moment of inertia with mass changes at 1.2 $M_\odot$ as a result of the switch from CNO cycle to *p-p* burning (Kawaler 1987). Whether real stars react to this structural change by a change in initial angular momenta, of by other means (increased stellar winds, e.g.), remains to be documented observationally. With these caveats we proceed to compare the rotational braking hypothesis with observations.

Once again, the principal observational evidence against the rotational braking explanation for the Li dip lies in the well-defined Hyades Li dip. While the distribution of rotational velocities in the higher mass stars does appear Maxwellian (Deutsch 1970), there are slow and intermediate rotators among them. Thus, while the high-mass stars may, *on average*, undergo a greater magnitude of spin-down and thus undergo larger amounts of Li depletion than stars of lower mass, the slow rotators among them will remain undepleted. If the observed spread in v sin i in the Hyades Li dip stars (10–60 km s^{-1}) is representative of the initial spread in velocities of these stars, then the Li dip should not be as well defined as is observed. The Hyades upper envelope is nicely fit by $J_0 = (1.6\text{–}5.0) \times 10^{49}$ g cm^2 s^{-1} in Figure 15 of Pinsonneault et al. (1990). To fit the Hyades dip with the Pinsonneault et al. (1990) model, one would have to assume that none of the stars in the dip had J_0 in this range. Such an argument must be extended to all of the other clusters as well. *The absence of stars with little or no depletion in the temperature of the Li dip in all of the observed clusters is a strong case against the rotational braking model as an explanation for the Li dip.* This is not to imply that rotational braking is not, perhaps, the cause of Li depletion at lower masses since the existing data are not inconsistent with their predictions. Nor even is it to imply that rotational braking as described by Pinsonneault et al. (1990) does not affect Li abundances in the dip stars. In fact, the spread in Li seen in III-57 and neighboring stars in the M67 dip and hinted

at in stars near the bottom of the Hyades dip may result from such initial angular momentum differences. A reasonable assumption is that the dip stars had a spread in initial angular momentum of about a factor of 10, similar to the spread seen in the Hyades dip stars and in lower mass stars in younger clusters. It then appears that independent of its initial angular momentum, a star which is at the temperature of the Li dip finds its Li to be inexorably destroyed.

5.2.4. *Observational Clues about Rotation and the* Li *Dip*

A comparison of two previous observational studies suggests that the rotational evolution of the dip stars may hold the clue to their anomalous Li depletion. Boesgaard (1976b) noted that the rise in Li on the cool side of the Hyades dip is coincident in temperature with a sharp drop in rotational velocities (the rotational break). Boesgaard's (1987b) result is reproduced in Figure 13 with our revised temperatures and Li abundances. Rotational velocities for the F stars are taken from Kraft (1965) and for the G stars from Radick et al. (1987).

Balachandran (1990a) pointed out that a similar correlation is not seen in field F stars. On the H-R diagram the rotational break was seen at $\sim 1.4\ M_{\odot}$, and the blue edge of the Li dip at $\sim 1.35\ M_{\odot}$. A band of slow rotators with normal Li clearly separated these two groups (see Fig. 6 in Balachandran 1990a). Balachandran (1990a) derived masses and ZAMS temperatures for the field F stars using a procedure similar to ours. Li abundances and rotational velocities for F stars with $-0.1 > [\mathrm{Fe/H}] > -0.3$ are reproduced from that study in Figure 14. This metallicity range is chosen because it provides the largest sample, but similar distributions of Li and v sin i with ZAMS $T_{\rm eff}$ are seen at other metallicities as well. In order to reduce uncertainties in masses and ZAMS temperatures, only stars which have evolved past the blueward hook on the H-R diagram are included. Despite this care, the inhomogeneous field star sample does not produce as well defined a Li dip as in the clusters.

While the Hyades dip stars rotate with v sin i's of 10–60 km s^{-1} and the rotational break in coincident with the Li dip, the field dip stars rotate with v sin i's not exceeding 20 km s^{-1}, and the rotational break is not seen until temperatures hotter than the blue end of the dip. We caution against a direct comparison of the v sin i distributions in the Hyades and field stars since Balachandran (1990a) used the Vandenberg (1985) grid of evolutionary tracks to derive ZAMS temperatures.

These observations raise interesting questions about the evolution of the rotational velocities of the dip stars. Comparisons of clusters of different ages have shown that the surfaces of G and K dwarfs spin down relatively quickly after their arrival on the main sequence, from velocities of up to 200 km s^{-1} in the 50 Myr α Persei cluster to velocities of less than 10 km s^{-1} in the 750 Myr Hyades. In the initial spin-down phase, comparison of α Persei with the slightly older 70 Myr Pleiades cluster suggests that G dwarfs spin down more rapidly than K

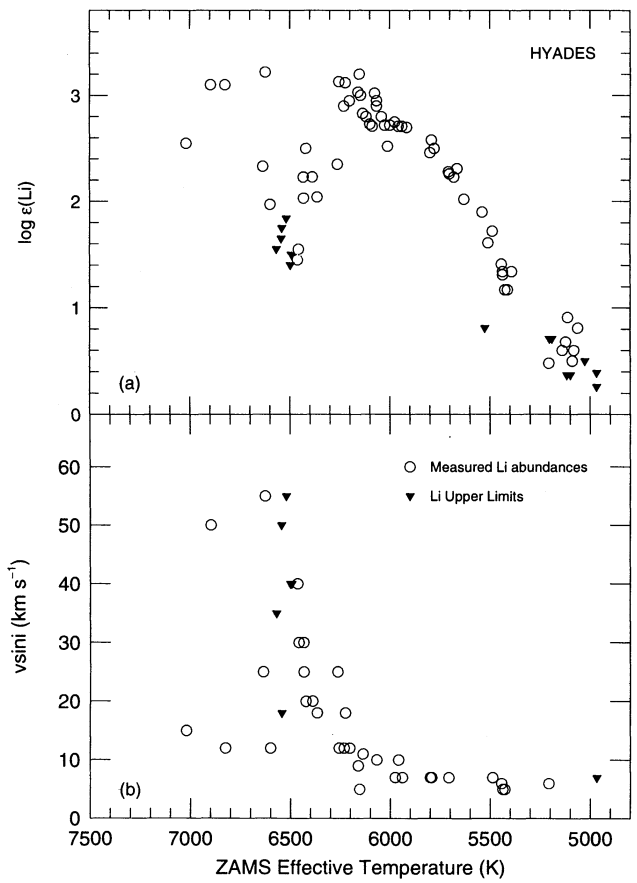

FIG. 13.—(*a*) Li abundances and (*b*) v sin i as a function of ZAMS $T_{\rm eff}$ in the Hyades. In each plot, circles represent measured Li abundances, and triangles Li upper limits. This is similar to the plot in Boesgaard (1987b) but uses our revised temperature scale and abundances. Rotational velocities were taken from Kraft (1965) and Radick et al. (1987).

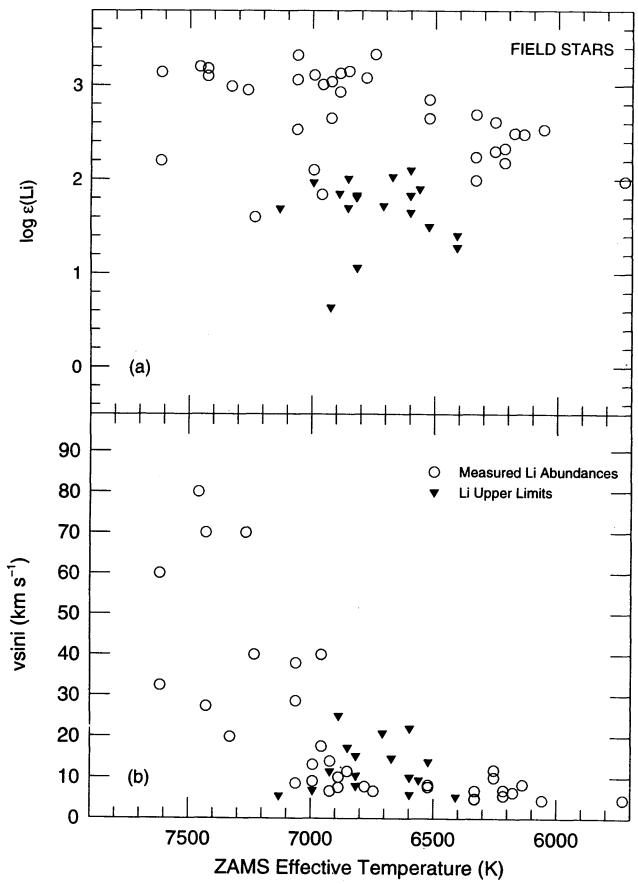

FIG. 14.—(*a*) Li abundances and (*b*) v sin i as a function of ZAMS $T_{\rm eff}$ for field F stars with $-0.1 > [\mathrm{Fe/H}] > -0.3$. In each plot, circles represent measured Li abundances, and triangles Li upper limits. The data were taken from Balachandran (1990a).

dwarfs, and this has been attributed to the smaller mass fraction in their convective envelopes (see Stauffer 1991, and references therein). At the age of the Hyades, the G dwarfs have velocities of ~ 10 km s^{-1} compared to 5 km s^{-1} in the K dwarfs (Radick 1987). Given this scenario, one expects the F dwarfs with extremely thin convective envelopes to spin down almost instantaneously on arrival on the main sequence, and the rotational break, which divides stars which do and do not undergo spin-down, to be established well before the age of the Hyades. Comparison of the Hyades and field star velocities raises the possibility that the mid-F stars in the Li dip do undergo spin-down but on a very long timescale, with the rotational break slowly moving blueward with age.

In order to explore that possibility, it is necessary to understand the evolutionary status of the two samples of stars. The Hyades dip stars are essentially very close to their ZAMS positions. On the other hand, the field stars (age ~ 3–4 Gyr) are located just past the blue hook on the H-R diagram and are poised to evolve horizontally across the Hertzsprung gap. While the ZAMS temperatures of typical field dip stars are between 6500 and 7000 K, their present temperatures range between 6200 and 6600 K. Has this redward evolution, which moves the stars into the region of more rapid braking, resulted in their slower velocities?

Redward evolution has occurred at two phases for the F dwarfs: on the main sequence and just past the blue hook phase. We contend that braking is not likely to have occurred past the blueward hook phase for two reasons: (1) stars at a similar evolutionary phase and effective temperature, but slightly more massive than the dip have a large range in rotational velocities similar to their main-sequence progenitors (see Fig. 6 in Balachandran 1990a), and (2) the low rotational velocities characteristic of all subgiants are not seen until later spectral types around G0 (Gray 1989; de Medeiros & Mayor 1990). Braking due to redward evolution on the main sequence, however, remains a distinct possibility which cannot be addressed by the Hyades and field star data alone.

Such braking is best tested by examining the rotational velocity distribution in a cluster older than the Hyades; NGC 752 is the ideal candidate. While some $v \sin i$ measurements were reported by Hobbs & Pilachowski (1986a) for a subset of the NGC 752 members with measured Li abundances, the data are sparse. Velocities of 20–40 km s^{-1} are seen in five stars in the Li dip. Based on this small sample the velocity range of the dip stars appears to be larger than in the field stars. While none of the stars have velocities as large as in the Hyades, additional data are clearly required to establish the rotational velocity distribution. Of course, the position of the rotational break cannot be placed definitively with this small sample. The crucial parameter which probably determines whether significant braking occurs during the main-sequence phase is the duration the star spends at a temperature significantly cooler than the ZAMS temperature. According to the RYI isochrones, the typical dip star in NGC 752 at 6500 K and 2 Gyr has not evolved redward, but has evolved blueward to a temperature ~ 50 K hotter than the ZAMS temperature from which it originated. Evolutionary effects are hence minimal in the NGC 752 Li dip stars, but the difference in age between the Hyades and NGC 752 is substantial enough to look for effects of braking at the temperature of the Li dip.

Conclusive determination of a lower mean rotational velocity in NGC 752 relative to the Hyades would strongly suggest a blueward movement of the rotational break with age and indicate a slow surface spin-down of the dip star, in contrast to the rapid surface spin-down of late-F and G dwarfs. The long timescale for surface spin-down may point to weak stellar winds and indicate that the efficiency of angular momentum loss from the surface equals the efficiency of transport from the interior. Surface spin-down on such a long timescale could conceivably result in greater mixing.

5.3. *Mass Loss*

Based on the rough coincidence between the instability strip and the position of the Li dip (the red edge of the instability strip is actually bluer than the Li dip) Schramm, Steigman, & Dearborn (1990) suggested that pulsation-driven mass loss was the cause of the Li dip. Using the observational evidence that the Li dip is strong but no Be depletion is detected in the Hyades, they obtain stringent constraints of $0.7 \times 10^{-10}\ M_\odot$ yr$^{-1} \leq \dot{M} \leq 1.0 \times 10^{-10}\ M_\odot$ yr^{-1} on the mass-loss rate. While the cluster data discussed here are not inconsistent with their arguments, their hypothesis is in severe disagreement with several sets of observations published since their study.

Since the convective zone in Population I F dwarfs is only a few percent by mass of the Li and Be preservation zones, no Li depletion will be perceived in the mass-losing model until the convective zone reaches the bottom of the Li preservation zone, at which time Li depletion will be extremely rapid. Yet observations indicate that the Li dip forms gradually. While it may be debated whether the dip is indeed seen at an incipient stage in the Pleiades, Balachandran (1991b) measured a factor of 10 depletion at the bottom of the Li dip in the 200 Myr old cluster NGC 6475. According to the mass-loss rate of Schramm et al. (1990), the F star in NGC 6475 would have lost at most 0.02 $M_\odot$, and since, by their own calculations, the Li preservation zone is 0.05 $M_\odot$, no depletion is predicted by their models at this age.

Deliyannis & Pinsonneault (1993) cite several field F dwarfs at the temperature of the Li dip which show both Li and Be to be depleted. Their point of contention with the mass-loss model is that both Li and Be, though depleted, are measurable in these stars. Since the Be preservation zone is deeper than the Li preservation zone, Be depletion, according to the mass-loss model, should not occur until all of the Li has been destroyed.

Finally, a recent examination of δ Scuti stars, which should have undergone mass loss since they reside in the instability strip, shows no evidence for Li depletion (Russell 1995). Thus mass loss is not a suitable explanation for the Li dip.

6. SUMMARY

One goal of this study was to examine the depth of mixing in the Li dip stars by studying subgiants and giants which have evolved from the Li dip. The old open cluster M67 provides the ideal site, and our observations have firmly established that the stars in the Li dip have undergone severe destruction of Li. Since there is no evidence for Li dredge-up in the subgiants or giants, mixing has occurred to depths hot enough to burn Li.

The second goal was to compare the Li dip in M67 with those in younger clusters: the Hyades, Praesepe, and NGC 752, to examine the evolutionary behavior of the dip and to look for variations with metallicity. In order to accomplish this, a uniform temperature calibration was required. It was shown that extrapolation of the C^3 Hyades calibration beyond 6500 K results in temperatures which are too hot and thus alters the shape of the Li dip. While we have adopted the SH calibration as the more accurate temperature estimator for

$B-V \leq 0.63$, additional high-resolution spectra of Hyades members between 6600 and 7200 K are required to provide a spectroscopic check on this and other calibrations. The Böhm-Vitense (1981) calibration was used for $B-V > 0.63$. Temperatures were reestimated, and published equivalent widths were reanalyzed to obtain a uniform set of Li abundances for all clusters.

This reanalysis of the published cluster data illustrates the need for the use of a consistent and well-understood temperature calibration and standardized abundance analyses before comparisons of clusters of different ages and metallicities can be carried out. The Li distributions in the Hyades and Praesepe G dwarfs were found to be identical, in contradiction to earlier suggestions by Soderblom et al. (1993a). The reanalysis also shows that vB 62, the short-period binary in the Hyades, does not have an anomalously high Li abundance as claimed previously by Soderblom et al. (1990) and Thorburn et al. (1993). The SH temperature calibration and revised abundance analysis equalizes the upper Li envelopes on the hot and cool sides of the Hyades dip and places the Li abundance at a value consistent with the meteoritic value.

Comparison of the Li dips in the four clusters reveals that the mass of the Li dip increases with increasing metallicity, but the ZAMS temperature from which the dip has originated is independent of metallicity. The detection of Li at $\log \epsilon(\mathrm{Li}) = 1.0$ in one M67 subgiant at 0.35 dex larger than upper limits placed on stars at similar evolutionary phases argues for the existence of a spread in Li within the Li dip. The morphology of the Li dip is characterized by a sharp drop at the blue edge and a more gradual rise at the red edge. While no change in the ZAMS temperature or shape of the blue edge is seen with age, the red edge becomes less steep with age. This may either result from an evolution in the Li dip, or be caused by a decrease in Li in stars cooler than the red edge and thus unrelated to the Li dip phenomenon. The shape of the Li dip is identical in the Hyades and Praesepe in the Li versus T_{eff} plane indicating that it is independent of the metallicity of the cluster.

Existing theoretical explanations were examined in the light of our analysis. While microscopic diffusion remains the most simple explanation for the Li dip, various circulation and turbulence calculations have called its effectiveness into question. The absence of detectable Li in all but one of the M67 subgiants and giants is a serious observational contradiction of the microscopic diffusion hypothesis. Mass loss, as an explanation for the Li dip, is shown to be in conflict with existing data. A number of the remaining models invoke rotation as the source of mixing. While a combination of microscopic diffusion and meridional circulation can be made to account for the Li dip, mixing through meridional circulation would predict large Li underabundances in rapidly rotating stars more massive than the Li dip, which are not observed. Turbulent diffusion models have been tailored to account for the dip and so must be tested against other predictions, e.g., $^{12}C/^{13}C$ ratios in giants. Rotational braking has been suggested as a means for producing the large Li depletion in the Li dip, but these models rely upon a sharp change in the initial angular momenta of stars at the cool edge of the Li dip which remains to be documented observationally. Due to the rotational velocity range seen explicitly in the Hyades dip stars, all of the models invoking rotation will probably produce a larger scatter in Li in the dip than is observed.

Previous observational studies have revealed that the Li and $v \sin i$ distributions in the Hyades and in field stars differ significantly from each other. We suggest that this may be an indication that the rotational break moves blueward with age. In order to establish that the slower rotation of the more evolved field stars is not merely a result of their redward evolution off the main sequence, a detailed examination of the $v \sin i$ distribution of Li dip stars in NGC 752 is required. Confirmation of this hypothesis would indicate that the surfaces of the dip stars spin down on a much longer timescale than late-F and G dwarfs and may hold the clue to anomalous mixing which occurs only in this narrow temperature interval.

I would like to thank the Margaret Cullinan Wray Charitable Lead Annuity Trust for its support of the American Astronomical Society Small Research Grant Program which funded travel to the observatories and made this work possible. Thanks are also due to Andy McWilliam for obtaining a few of the early M67 spectra, John Carr and Marc Pinsonneault for numerous discussions, Bengt Edvardsson for discussions on the EAGLNT temperature calibration, and David Lambert and Bruce Carney for their careful reading of the manuscript. This work was supported in part by NSF grant AST 92-21711.

REFERENCES

Anders, E., & Grevesse, N. 1989, Geochim. Cosmochim. Acta, 53, 197
Andersen, J., Gustafsson, B., & Lambert, D. L. 1984, A&A, 136, 65
Balachandran, S. 1988, Ph.D. thesis, Univ. Texas
———. 1990a, ApJ, 354, 310
———. 1990b, in ASP Conf. Ser., 9, Proc. 6th Cambridge Workshop on Cool Stars, Stellar Systems and the Sun, ed. G. Wallerstein (San Francisco: ASP), 357
———. 1991a, Mem. Soc. Astron. Italiana, 62, 33
———. 1991b, in ASP Conf. Ser., 40, Inside the Stars, ed. W. W. Weiss & A. Baglin (IAU Coll. 137) (San Francisco: ASP), 333
Balachandran, S., Lambert, D. L., & Stauffer, J. R. 1988, ApJ, 333, 267
Bell, R. A., Eriksson, K., & Gustafsson, B. 1990, private communication
Bell, R. A., Eriksson, K., Gustafsson, B., & Nordlund, Å. 1976, A&AS, 23, 37
Biémont, E., Badoux, M., Kurucz, R. L., Ansbacher, W., & Pinnington, E. H. 1991, A&A, 249, 539
Blackwell, D. E., & Lynas-Gray, A. E. 1994, A&A, 282, 899
Blackwell, D. E., Lynas-Gray, A. E., & Petford, A. D. 1991, A&A, 245, 567
Blackwell, D. E., Petford, A. D., Arribas, S., Haddock, S. J., & Selby, M. J. 1990, A&A, 232, 396
Blackwell, D. E., & Shallis, M. J. 1977, MNRAS, 188, 847
Boesgaard, A. M. 1987a, ApJ, 321, 967
———. 1987b, PASP, 99, 1067
———. 1989, ApJ, 336, 798
Boesgaard, A. M., & Budge, K. G. 1988, ApJ, 332, 410 (BB)
Boesgaard, A. M., & Tripicco, M. J. 1986, ApJ, 302, L49 (BT)
Böhm-Vitense, E. 1981, ARA&A, 19, 295
Bouvier, J. 1991, in Formation and Evolution of Low Mass Stars, ed. S. Catalano & J. R. Stauffer (Dordrecht: Kluwer), 41
Burkhart, C., & Coupry, M. F. 1989, A&A, 197, 205
———. 1991, A&A, 249, 205
Carney, B. W. 1983, AJ, 88, 623
Carney, B. W., Latham, D. W., Laird, J. B., & Aguilar, L. A. 1994, AJ, 107, 2240
Cayrel, R., Cayrel de Strobel, G., & Campbell, B. 1985, A&A, 146, 249 (C^3)
Cayrel de Strobel, G. 1990, Mem. Soc. Astron. Italiana, 61, 613
Charbonneau, P., & Michaud, G. 1988, ApJ, 334, 746
———. 1990, ApJ, 352, 681
Charbonneau, P., Michaud, G., & Proffitt, C. R. 1989, ApJ, 347, 821
Charbonnel, C. 1994, A&A, 282, 811
Charbonnel, C., & Vauclair, S. 1992, A&A, 265, 55
Charbonnel, C., Vauclair, S., & Zahn, J.-P. 1992, A&A, 255, 191
Code, A. D., Davis, J., Bless, R. C., & Hanbury Brown, R. 1976, AJ, 203, 417
Cohen, J. G., Frogel, J. A., & Persson, S. E. 1978, ApJ, 222, 165
Daniel, S. A., Latham, D. W., Mathieu, R. D., & Twarog, B. A. 1994, PASP, 106, 281
Deliyannis, C. P., & Pinsonneault, M. H. 1993, in ASP Conf. Ser., 40, Inside the Stars, ed. W. W. Weiss & A. Baglin (IAU Coll. 137) (San Francisco: ASP), 174
Demarque, P., Green, E. M., & Guenther, D. B. 1992, AJ, 103, 151

de Medeiros, J. R., & Mayor, M. 1990, in ASP Conf. Ser., 9, Proc. 6th Cambridge Workshop on Cool Stars, Stellar Systems and the Sun, ed. G. Wallerstein (San Francisco: ASP), 404
Deutsch, A. J. 1970, in Stellar Rotation, ed. A. Slettebak (Dordrecht: Reidel), 207
Eddington, A. S. 1925, Observatory, 48, 78
Edvardsson, B., Andersen, J., Gustafsson, B., Lambert, D. L., Nissen, P. E., & Tomkin, J. 1993, A&A, 275, 101
Eggen, O. J., & Sandage, A. R. 1964, ApJ, 140, 130
Endal, A. S., & Sofia, S. 1981, ApJ, 220, 279
Fagerholm, E. 1906, Inaugural diss., Uppsala
Fekel, F. C., & Balachandran, S. 1993, ApJ, 403, 708
Friel, E. D., & Boesgaard, A. M. 1992, ApJ, 387, 170
García López, R. J., Rebolo, R., & Beckman, J. E. 1988, PASP, 100, 1489
García López, R. J., & Spruit, H. C. 1990, ApJ, 377, 268
Gaupp, A., Kuste, P., & Andra, H. J. 1982, Phys. Rev. A, 26, 3551
Gilroy, K. K. 1988, Ph.D. thesis, Univ. Texas
———. 1989, ApJ, 347, 835
Gray, D. F. 1989, ApJ, 347, 1021
Green, E. M., Demarque, P., & King, C. R. 1987, The Revised Yale Isochrones and Luminosity Functions (New Haven: Yale Univ. Obs.)
Grevesse, N., Lambert, D. L., Sauval, A. J., van Dishoeck, E. F., Farmer, C. B., & Norton, R. H. 1990, A&A, 232, 225
———. 1991, A&A, 242, 488
Grevesse, N., & Noels, A. 1993, in Origin and Evolution of the Elements, ed. N. Prantzos, E. Vangioni-Flam, & M. Casse (Cambridge: Cambridge Univ. Press), 15
Griffin, R. F., & Gunn, J. E. 1978, AJ, 83, 1114
Griffin, R. F., Gunn, J. E., Zimmerman, B. A., & Griffin, R. E. M. 1988, AJ, 96, 172
Gustafsson, B., Bell, R. A., Eriksson, K. E., & Nordlund, A. 1975, A&A, 42, 407
Heinemann, R. 1926, AN, 227, 213
Hobbs, L. M., & Pilachowski, C. 1986a, ApJ, 309, L17
———. 1986b, ApJ, 311, L37
———. 1988, ApJ, 334, 734
Hobbs, L. M., & Thorburn, J. A. 1991, AJ, 102, 1070
Holweger, H., Bard, A., Kock, A., & Kock, M. 1991, A&A, 249, 545
Huebner, W. F., Merts, A. L., Magee, N. H., & Argo, M. F. 1977, Los Alamos Sci. Lab. Rep. LA-6760-M
Iben, I., Jr. 1967, ApJ, 147, 624
Johnson, H. L. 1952, ApJ, 116, 640
———. 1957, ApJ, 126, 121
Johnson, H. L., & Knuckles, C. F. 1955, ApJ, 122, 209
Kawaler, S. D. 1987, PASP, 99, 1322
Klein-Wassink, W. J. 1927, Groningen Publ. 41
Kraft, R. P. 1970, in Spectroscopic Astrophysics, ed. G. Herbig (Berkeley: Univ. California Press), 385
Kurucz, R. L. 1979, ApJS, 40, 1
———. 1990, in Atomic Spectra and Oscillator Strengths for Astrophysics and Fusion Research, ed. J. E. Nansen (Amsterdam: North-Holland), 20
Kurucz, R. L., Furenlid, I., Brault, J., & Testerman, L. 1984, Solar Flux Atlas from 296 to 1200 Nanometers (Tucson: National Solar Obs.)
Kurucz, R. L., & Peytremann, E. 1975, Smithsonian Astrophys. Obs. Spec. Rep. 362
Lemoine, M., Ferlet, R., Vidal-Madjar, A., Emerich, C., & Bertin, P. 1993, A&A, 269, 469
Mathieu, R. D., Latham, D. W., & Griffin, R. F. 1990, AJ, 100, 1859
Mathieu, R. D., Latham, D. W., Griffin, R. F., & Gunn, J. E. 1986, AJ, 92, 1100
Mathis, J. S. 1990, ARA&A, 28, 37
Mendoza, E. E. 1967, Bol. Obs. Tonantzintla y Tacubaya, 4, 149
Michaud, G. 1986, ApJ, 302, 650
Montgomery, K. A., Marschall, L. A., & Janes, K. A. 1993, AJ, 106, 181
Nissen, P. E., Twarog, B. A., & Crawford, D. L. 1987, AJ, 93, 634
Pilachowski, C. 1986, ApJ, 300, 289
Pilachowski, C. A., & Hobbs, L. M. 1988, PASP, 100, 336
Pilachowski, C. A., Saha, A., & Hobbs, L. M. 1988, PASP, 100, 474
Pinsonneault, M. H., Kawaler, S. D., & Demarque, P. ApJS, 74, 501
Pinsonneault, M. H., Kawaler, S. D., Sofia, S., & Demarque, P. 1989, ApJ, 338, 424
Proffitt, C. R., & Michaud, G. 1991, 371, 584
Radick, R. R., Thompson, D. T., Lockwood, G. W., Duncan, D. K., & Baggett, W. E. 1987, ApJ, 321, 459
Randich, S., Gratton, R., & Pallavicini, R. 1993, A&A, 273, 194
Richer, J., & Michaud, G. 1993, ApJ, 416, 312
Richer, J., Michaud, G., & Proffitt, C. R. 1992, ApJS, 82, 329
Ridgway, S. T., Joyce, R. R., White, N. M., & Wing, R. F. 1980, ApJ, 235, 126
Rodgers, F. J., & Inglesias, C. A. 1992, ApJS, 79, 507
Russell, S. 1995, in Proc. ESO/EPIC Workshop on the Light Element Abundances, ed. P. Crane (New York: Springer), in press
Sanders, W. L. 1977, A&AS, 27, 89
Saxner, M., & Hammarbäck, G. 1985, A&A, 151, 372 (SH)
Schramm, D. N., Steigman, G., & Dearborn, D. S. P. 1990, ApJ, 359, L55
Schwan, H. 1991, A&A, 243, 386
Sneden, C. 1973, Ph.D. thesis, Univ. Texas
Soderblom, D. R., Fedele, S. B., Jones, B. F., Stauffer, J. R., & Prosser, C. F. 1993a, AJ, 106, 1080
Soderblom, D. R., Jones, B. F., Balachandran, S., Stauffer, J. R., Duncan, D. K., Fedele, S. B., & Hudon, J. D. 1993b, AJ, 106, 1059
Soderblom, D. R., Oey, M. S., Johnson, D. R. H., & Stone, R. P. S. 1990, AJ, 99, 595
Soderblom, D. R., Pilachowski, C. A., Fedele, S. B., & Jones, B. F. 1993c, AJ, 105, 2299
Soderblom, D. R., Stauffer, J. R., Daniel Hudon, J., & Jones, B. F. 1993d, ApJS, 85, 315
Spite, F., Spite, M., Peterson, R. C., & Chaffee, F. H. 1987, A&A, L8
Stauffer, J. R. 1991, in Formation and Evolution of Low Mass Stars, ed. S. Catalono & J. R. Stauffer (Dordrecht: Kluwer), 151
Sweet, P. A. 1950, MNRAS, 110, 548
Swenson, F. J., Faulkner, J., Iglesias, C. A., Rogers, F. J., & Alexander, D. R. 1994, ApJ, 422, L79
Tassoul, J.-L., & Tassoul, M. 1982, ApJS, 49, 317
Thorburn, J. A., Hobbs, L. M., Deliyannis, C. P., & Pinsonneault, M. H. 1993, ApJ, 415, 150
Tull, R. G., MacQueen, P., Sneden, C., & Lambert, D. L. 1994, in ASP Conf. Ser., 55, Optical Astronomy from the Earth and Moon, ed. D. M. Pyper & R. J. Angione (San Francisco: ASP), 148
van Bueren, H. G. 1952, Bull. Astron. Inst. Netherlands, 11, 385
Vandenberg, D. A. 1985, ApJS, 58, 711
Vauclair, S. 1988, ApJ, 335, 971
Wallerstein, G., Herbig, G. H., & Conti, P. S. 1965, ApJ, 141, 610